



Short-term effect of liquid organic fertilisation and application methods on N₂, N₂O and CO₂ fluxes from a silt loam arable soil

Balázs Grosz¹ · Stefan Burkart¹ · Reinhard Well¹

Received: 28 September 2023 / Revised: 14 March 2024 / Accepted: 17 March 2024
© The Author(s) 2024

Abstract

The absence of N₂ flux measurements in liquid manure-amended soils has resulted in a poor understanding of the effect of manure application on gaseous N losses. The aim of this study was to quantify N₂, N₂O, CO₂, N₂O reduction to N₂, depth distribution of moisture, water-extractable organic C, NO₃⁻, NH₄⁺, pH, and diffusivity in a laboratory incubation experiment with an arable silt-loam soil. To quantify N processes and gaseous fluxes, ¹⁵N tracing was applied. An artificial livestock slurry-mixture was added to the soil in various treatments (control, surface or injected application; slurry-application rate: 42.9 kg N ha⁻¹; soil water content of either 40% or 60% water-filled pore space (WFPS)). The soil was incubated for 10 days. The depth distribution of the control parameters was measured twice during the experiment on days 5 and 10. The average increase in N₂ and N₂O fluxes from denitrification was about 900% in slurry-amended soils. The highest N₂ and N₂O fluxes from denitrification were measured in the slurry injection, 60% WFPS treatment (7.83 ± 3.50 and 11.22 ± 7.60 mg N m⁻² d⁻¹, respectively). The hypothesis that injected slurry at a higher water content enhances denitrification was confirmed. This study provides important insights into the formation, spatial and temporal variation of the manure-soil hotspot and its impact on the denitrification process. The results will form part of a dataset to develop, improve and test manure application submodules of biogeochemical models and will help to understand in detail the effect of hotspots on N-cycling in manure-treated soils.

Keywords Manure · Hotspot · Denitrification · Nitrification · ¹⁵N · Incubation

Introduction

The world's continuously growing population is increasing the demand for greater agricultural production efficiency, which means that more N fertiliser is being applied (Erisman et al. 2011). In addition, current global diet trends are resulting in greater consumption of animal products, which in turn is leading to a rise in the number of livestock (Bernal et al. 2015; Buckwell and Nadeu 2016). There is therefore an urgent need to optimise manure fertilisation as regards nutrient efficiency and its environmental impact (Königer et al. 2021). However, organic fertilisation could lead to considerable N losses and carries a potential environmental risk (Galloway et al. 2004).

Nitrate (NO₃⁻) leaching and gaseous N losses weaken N use efficiency (NUE), with the implication that crop yields are reduced. In addition, the gaseous N losses of applied fertilisers, such as ammonia (NH₃), nitric oxide (NO) and nitrous oxide (N₂O), contribute to the acidification of unmanaged waters and soils, air pollution and global warming (Galloway et al. 2004).

Nitrous oxide is a stratospheric ozone-depleting substance and a potent greenhouse gas (Ravishankara et al. 2009). The origin of a significant source (~52%) of anthropogenic N₂O in the atmosphere is direct emission from agricultural soils fertilised with mineral and organic fertilisers, livestock manure and aquaculture (Flessa et al. 2014; Tian et al. 2020; Malyan et al. 2021a, b).

The microbial soil processes of nitrification and denitrification are the main sources of the N₂O produced. The magnitude of the N₂O flux depends on the abundance of decomposable soil organic matter (Burford and Bremner 1975; Gilmour 1984; de Catanzaro and Beauchamp 1985; Bijay-singh et al. 1988; McCarty and Bremner 1993;

✉ Balázs Grosz
balazs.grosz@thuenen.de

¹ Thünen Institute of Climate-Smart Agriculture,
38116 Braunschweig, Germany

Groffman et al. 2009) and the availability of N substrates such as NO_3^- (Heinen 2006; Groffman et al. 2009) or ammonium (NH_4^+) (Malhi and McGill 1982; Gilmour 1984; Sahrawat 2008). Other control factors of the N_2O flux from nitrification and denitrification are temperature (Rodrigo et al. 1997; Sahrawat 2008), pH (Peterjohn 1991; Šimek and Hopkins 1999; Šimek and Cooper 2002; Sahrawat 2008), soil gas diffusivity (Balaine et al. 2013) and oxygen (O_2) concentration in the soil pore space (Sahrawat 2008; Müller and Clough 2014). In well-aerated, dry soils, it is mostly aerobic processes that are dominant, and these conditions favour nitrification and inhibit denitrification (Robertson and Groffman 2015). In contrast, anaerobic processes are mostly formed in soil domains with low gas diffusivity conditions, supporting denitrification and inhibiting nitrification (Stepniewski 1980; Petersen et al. 2013; Robertson and Groffman 2015). Nitrous oxide is an intermediate product of denitrification and it can be reduced to dinitrogen (N_2) as the final step of denitrification. Therefore, under denitrifying conditions, N_2O flux and $\text{N}_2\text{O}/(\text{N}_2 + \text{N}_2\text{O})$ product ratio (N_2O_i) are regulated by N_2O reduction to N_2 .

To minimise the negative effects (e.g. NH_3 losses, N_2O flux) and increase the NUE of organic fertiliser application, the application rate of nutrients per unit area, application time and also application technique are regulated (Federal Ministry of Justice and Consumer Protection 2017; Köninger et al. 2021). Thus, manure application in agricultural soils increases N_2O and N_2 fluxes, resulting in lower N use efficiency (NUE) and higher fertiliser-related N_2O fluxes compared with mineral N fertilisation (Ravishankara et al. 2009). Manure application affects nitrification and denitrification processes through the infiltration of manure water into the soil. This infiltration simultaneously transports mineral and labile organic N and labile organic carbon (C), resulting in increased O_2 consumption during the respiratory decomposition of the latter (Petersen et al. 1996; Sahrawat 2008; Markfoged et al. 2011; Zhu et al. 2014; Grosz et al. 2022; Buchen-Tschiskale et al. 2023). This leads to the local simultaneous occurrence of anoxia and high NO_3^- concentration from nitrification of slurry-derived NH_4^+ in the boundary zone between the soil and the manure clump. In addition, manure generally has higher water retention than the surrounding soil, resulting in the manure clump having a higher water content (Petersen et al. 2003). These factors may increase the rate of denitrification (Petersen et al. 2016). The reduction of the N_2O produced could be inhibited by low pH due to acidification from prior nitrification of manure-derived NH_4^+ and a high NO_3^- concentration locally, which can result in highly variable N_2O_i .

There are several sources and forms of applied liquid organic fertiliser in Germany, such as pig and cattle manure or biogas digestates from varying feedstocks (Hey et al.

2015). These are essential N sources for agriculture, where about half of the available N is in mineral form, mostly NH_4^+ (Sommer et al. 2004; Baral et al. 2016), and the other half is organic.

Different slurry incorporation techniques significantly impact gaseous N losses (Baral et al. 2016; Petersen et al. 2016). The effects of liquid manure incorporation techniques on N_2O fluxes have already been researched (Baral et al. 2016; Petersen et al. 2016). However, the application of liquid organic manure to agricultural soils leads to the formation of a hotspot in the manure-soil boundary layer, which has a significant impact on the complete denitrification process ($\text{N}_2 + \text{N}_2\text{O}$ fluxes) (John et al. 1989; Zhang et al. 2019), its intensity and product ratio. The description of these effects and the processes and factors influencing them in the literature is very limited. While NH_3 fluxes following slurry application with varying application techniques have been extensively studied in the past (Huijsmans et al. 2003; Webb et al. 2010; Petersen and Sommer 2011; Pacholski 2016; Park et al. 2018), there are few data on slurry effects on N_2 and N_2O fluxes from denitrification (Nielsen et al. 1996; Grosz et al. 2022; Buchen-Tschiskale et al. 2023). Until now, there have been just a few experimental results that show and predict the impact of soil and slurry moisture, pH, soil texture, organic C and mineral N (Grosz et al. 2022). Application method, spatial distribution and the diverse physical and chemical composition of slurry offer a highly complex research topic. Biogeochemical models are useful tools to predict soil processes, e.g. N_2O fluxes. However, the calibration and validation of modelled denitrification rates are inadequate because gaseous products from denitrification, including N_2 , have not been measured (Nielsen et al. 1996; Groffman et al. 2009; Butterbach-Bahl et al. 2013; Köster et al. 2015; Fiedler et al. 2017; Grosz et al. 2022; Buchen-Tschiskale et al. 2023). To date, there have been just a few attempts to incorporate process dynamics of manure-amended soil (Probert 2004; Sommer et al. 2004; Li et al. 2012; IUSS Working Group WRB. 2015). Therefore, several important variables and processes are missing from current models: the spatial distribution of applied manure with its implication on spatial nitrification-denitrification dynamics and related controls, and the influence of manure quality. To date, process-based models have assumed homogenous soil layers and thus also homogenous distribution of the applied slurry. The manure's N, C and water content are added to the bulk values of N and C pools and soil water content (Li et al. 2012). This inaccurate and simplified process description of manure-amended soil can lead to inadequate model results. Therefore, the development of models to describe manure-related labile N, C and water-induced hotspots, including spatial manure dynamics,

is crucial, but their evaluation is not feasible without suitable measurements.

This study aimed to create an appropriate dataset for testing and developing new modeling approaches to describe the boundary layer processes between liquid artificial livestock slurry (hereinafter slurry) and soil. The importance of this work is given by the lack of knowledge about the slurry-soil interaction. The effect of hotspot formation on the denitrification process is not well understood, which is related to the spatial formation of the boundary layer by the hotspot, the change in concentration of water and substrates from the slurry (Petersen et al. 1996). The activation of the denitrification process by hotspots in slurry-treated soils and the change in product ratio can be interpreted from the results of the experiments. It provides information on the spatial distribution of the water and the substrates, which can be inferred from the hotspot formed by the slurry. The surface slurry treatment is analogous to a surface broadcast slurry application for a standard agricultural practice. To compare the amount of slurry applied per unit area between the surface and injected applications, the amount of slurry used in the injected treatment was equal to the amount of slurry applied in the surface application. It is important to note that the method of the injected slurry application is different from field application methods with respect to geometry of the slurry layer and the soil-slurry boundary in geometry. In both cases, the slurry was applied as a flat layer while in field-scale slurry injection the slurry fills a V-shaped open slit. There is certainly an effect of the different geometry on the processes involved, but the experimental data are used for model development. Since biogeochemical models are mostly 1-dimensional, the design of the experiment required a corresponding slurry-soil geometry. Thus the 1D layer geometry allow to evaluate spatial hotspot effect with 1D models. In this study, research was thus conducted on how slurry and its application methods affect N_2 , N_2O and CO_2 fluxes from agricultural soils and how this is associated with the spatial distribution of control variables. Previously, we had conducted a similar study with sandy arable soil (Grosz et al. 2022). To achieve generalizability of the phenomena observed, we here repeat that study design with silt loam arable soil.

Since our goal was to simulate the process dynamics in the initial phase after slurry application, when the effect of the presence of plants on the processes under study is negligible, the experiment was conducted without plants. Moreover, in order to obtain the necessary data sets to train the models step by step, it is important to exclude certain confounding factors (here: plant effects) to facilitate the model evaluation.

Therefore, the objectives of this study were to determine the hotspot effect of slurry on the product ratio, to identify the pathways of N_2O productions and to quantify N_2O reduction and the depth distribution of NO_3^- , NH_4^+ , moisture, pH, water-extractable organic C (WEOC) and the N_2 , N_2O , and CO_2 fluxes. It was hypothesised that the slurry-produced boundary effect (i) increases the water content, WEOC and pH locally around the slurry clump, (ii) increases the NO_3^- concentration in the layer and nearby layers of the slurry clump, (iii) increases N_2O and N_2 fluxes due to increased denitrification activity, (iv) results in a lower N_2O_i , and finally that (v) the injected slurry applications, compared with the surface treatments, result in higher denitrification rates and decreased N_2O_i .

Materials and methods

Soil selection, sampling and preparation

The soil was collected in the middle of October 2019 from an arable silt loam soil (referred to below as silt loam soil) located in the “Goldener Acker” research field of the University of Hohenheim, Germany (48°42,5'N, 9°12,5'E, 400 m asl). The site has a mean annual temperature of 10.8 °C and average yearly precipitation of 662 mm. The soil samples were taken after tillage following the harvest of winter rape. The field's typical crop rotation is winter rape, winter wheat and winter barley. The soil is a Haplic Luvisol (IUSS Working Group WRB. 2015). The first 5 cm of soil contained incorporated winter wheat straw residues that were not yet incorporated by tillage. This layer was removed prior to sampling to obtain soil with low amount of crop residues to facilitate subsequent sieving. We thus collected soil from the 5 to 20 cm layer that was regularly mixed by tillage and which was thus largely homogenous in biogeochemical properties. Random soil sampling took place from a 2 m² area. After field collection with spades and shovels, the soil was transported to the laboratory, air-dried, sieved to 10 mm, homogenised and stored in plastic boxes at 4 °C until use. The soil samples for the laboratory analyses were sieved to 2 mm. The main soil properties were: clay, 27%; silt, 71%; sand, 2%; bulk density (BD), 1.4 g cm⁻³; pH(CaCl₂), 6.7 ± 0.1; N_{total} , 0.15 ± 0.02%; C_{org} , 1.34 ± 0.19%; C/N ratio, 9.14; CEC, 0.13 mol kg⁻¹ (ten Huf et al. 2023). To exclude the phase of intensive respiration and mineralisation typically following rewetting, the soils were pre-incubated at 35% of maximum water-holding capacity (~30% WFPS) for two weeks at room temperature.

Laboratory incubation

Experimental design and incubation set-up

The inorganic N content of the pre-incubated soil was $22.3 \text{ mg NO}_3^- \text{-N kg}^{-1}$ dry soil and $1.4 \text{ mg NH}_4^+ \text{-N kg}^{-1}$ dry soil. After pre-incubation, a ^{15}N -labelled KNO_3 (98 atom% ^{15}N) solution was added to the soil at $46.8 \text{ mg N kg}^{-1}$ dry soil ($60.8 \text{ kg N ha}^{-1}$) and thoroughly homogenised by mixing. The N content and amount of water were selected to reach the target values of 65 atom% ^{15}N enrichment of the NO_3^- pool and the water content of the drier treatment.

A mesocosm incubation system was used, as described previously (Grosz et al. 2022). Briefly, pre-incubated and fertilised soil was placed in aluminium columns with an inner diameter of 9.4 cm and a height of 10 cm at a bulk density of 1.3 g cm^{-3} . These columns were then positioned within gas-tight Plexiglas® cylinders with an inner diameter of 14.4 cm and a height of 18 cm to measure the gas flux. Bulk density was determined by filling the 694 cm^3 aluminium column with 902.2 g of dry soil equivalent, and compacting it in a single layer using a lever press machine. For injected treatments, the soil was packed in two layers.

After filling the cylinders with soil, 13.9 g kg^{-1} artificial slurry mixture (Table S1), equivalent to 20.8 Mg ha^{-1} containing $42.9 \text{ kg N ha}^{-1}$ ($28.6 \text{ mg N kg}^{-1}$, comprising $19.3 \text{ mg NH}_4^+ \text{-N kg}^{-1}$) and $20 \text{ Mg H}_2\text{O ha}^{-1}$ (equivalent to $13.3 \text{ g H}_2\text{O kg}^{-1}$), was added to each soil core. Since varying the amount of slurry was beyond the scope of the experiment, the amount of slurry used in the study was set at the lower limit of the amount of slurry applied in the surface broadcast treatment in agricultural practice. To provide artificial slurry with a defined composition, 2.43 kg solid dairy cow faeces (Table S1) were mixed with a solution of 1.37 kg organic material (urea: 17.117 g dm^{-3} , hippuric acid: 4.095 g dm^{-3} , allantoin: 4.744 g dm^{-3} , uric acid: 0.330 g dm^{-3} , creatinine: 1.131 g dm^{-3} , all together: 4.76 g N dm^{-3}), inorganic salts (KHCO_3 : 14.0 g dm^{-3} , KCl : 10.5 g dm^{-3} , $\text{CaCl}_2 \cdot \text{H}_2\text{O}$: 0.4 g dm^{-3} , $\text{MgCl}_2 \cdot 5\text{H}_2\text{O}$: 1.2 g dm^{-3} , Na_2SO_4 : 3.7 g dm^{-3}) and 2.406 L water (Sørensen 1998; Kool et al. 2006). The proportions of a mixture of solid dairy cow faeces, artificial urine, and water were 49%, 27%, and 24%, respectively, following the proportions reported in Sørensen (1998). The fresh faeces were collected from dairy cows whose diet consisted of a total mixed ration containing grass silage and concentrates. The faeces were frozen at $-18 \text{ }^\circ\text{C}$ after sampling. The solid dairy cow faeces and salt solution mixtures were matured for 30 days at room temperature to imitate the common slurry storage practice, and then stored at $-18 \text{ }^\circ\text{C}$ until the experiment (Table S1). To mimic the surface and injected application of manure, the slurry was added as one layer at the top surface or at

5 cm soil depth, respectively. This method differs from the geometry of slot injection during field application since the experiment's results were to be used for the calibration and development of biogeochemical models. The placement and geometry of the added slurry were designed to apply 1D models (i.e. DNDC, DailyDayCent, Coupmodel and DeNi). It is important to note that the researched soil-manure boundary layer, as the hotspot contact area between the manure and the soil, is more relevant and essential than the geometry of the injected slot.

Two soil moisture levels were established, with the target water content represented as water-filled pore space (WFPS), which is defined as the volumetric water content of the pore volume, excluding any water added to the slurry. As a result, the effective water content of slurry treatments was higher than the defined WFPS level.

Six replicates were prepared for each of the six treatments: control at 40% WFPS (C40), control at 60% WFPS (C60), surface slurry treatment at 40% WFPS (S40), surface slurry treatment at 60% WFPS (S60), injected slurry treatment at 40% WFPS (I40) and injected slurry treatment at 60% WFPS (I60).

During the ten-day experiment, the moisture and temperature ($15 \text{ }^\circ\text{C}$) were kept at constant levels. To facilitate homogeneous compaction and maintain soil structure stability, soil was kept dry during packing, i.e. soils were placed in the cylinder and compacted at 40% WFPS (equivalent to 15.7 g g^{-1}). For the wet treatments, to achieve the target moisture content of 60% WFPS (equivalent to 23.5 g g^{-1}), additional water was added after column packing but before surface slurry application. The stratified slurry application was carried out as described by Grosz et al. (2022). Slurry was applied to the surface and to the center of the soil cores. In the latter case, half of the soil volume was compacted to a depth of 5 cm and slurry was applied to the surface of this lower part of the core, and the other half of the soil volume was then placed on top of the slurry layer and compacted to simulate slurry injection. To prevent blockage of soil-air gas exchange a small area along the soil edge (approximately 1 mm) was left free of slurry. The top layer and injected slurry layer received an identical amount of slurry equivalent to 20.8 t ha^{-1} (Table S1). The water content of the soil was adjusted to 15.7 g g^{-1} soil to achieve 40% WFPS and 23.5 g g^{-1} soil for 60% WFPS. This was equivalent to 14.2 and 21.2 g per soil layer of 1 cm thickness. The addition of the slurry mixture increased the water content of the slurry-amended soil layers through the addition of 13.9 g of water with the slurry, where this amount of water would double the water content of a 1 cm layer of 40% WFPS soil. The soil cylinders were incubated for ten days with continuous flushing of the headspace using an artificial gas mixture (2% N_2 , 20% O_2 , 320 ppb N_2O and 300 ppm CO_2 in He;

headspace volume: 2146.1 cm³) at a flow rate of 10 mL min⁻¹. The flow rates of each vessel were measured several times per day with a digital flow meter, and the actual flow was used to calculate gaseous N fluxes. CO₂ and N₂O were added to mimic assumed atmospheric levels, while the low N₂ concentration was used to enhance the sensitivity of isotope ratio mass spectrometry (IRMS) measurements (Lewicka-Szczebak et al. 2017).

Gas and stable isotope analysis

An automated incubation system was used for the incubation of the soil cylinders. Gas samples were analysed by a gas chromatograph (GC 2014; Shimadzu, Duisburg, Germany), with an electron capture detector (ECD), a flame ionisation detector (FID) and a thermal conductivity detector (TCD). After soil packing, the filled cylinders were almost immediately placed in the incubation system. The GC measured data points of CO₂ and total N₂O (N₂O_T; produced N₂O from all possible soil processes) in the first 16 h were omitted from the analyses. Using the GC, N₂O (total N₂O, N₂O_T), CH₄, N₂, and CO₂ concentrations were continuously measured in the outflow throughout the incubation (Hantschel et al. 1994; Säurich et al. 2019). Gas samples were also collected manually on days 1, 5 and 9 in 12 mL Exetainers with rubber septa (Labco Ltd., Lampeter, UK) for IRMS (MAT 253, Thermo Scientific, Bremen, Germany) analysis to determine the fluxes of N₂ (fp_N₂) and N₂O (fp_N₂O) originating from the ¹⁵N-labelled NO₃⁻ (Spott et al. 2006; Kemmann et al. 2021) (see the Supplementary Material for the calculation). Gas sampling was undertaken by connecting two 12 mL Exetainers from the outlet flow of the columns (Well et al. 2006). The Exetainer volume was exchanged approximately 1200 times before the samples were disconnected. The flux of N₂O from other sources was calculated by the difference between N₂O_T and fp_N₂O (N₂O_{os} = N₂O_T - fp_N₂O). Before measurement, the samples were handled using a modified GasBench II (Thermo Scientific, Bremen, Germany) for an analytical online preparation. A hot copper wire (650 °C) reduced the N₂O in the gas samples to N₂ in an oven. This copper wire is in the gas line between the GasBench II and IRMS (Lewicka-Szczebak et al. 2013). The

Table 1 Soil layer of destructive sampling

	Control	Surface	Injected
Number of layers	1	4	7
1	0–10 cm	0–1 cm	0–2.5 cm
2		1–2 cm	2.5–3.5cm
3		2–3 cm	3.5–4.5cm
4		3–10 cm	4.5–5.5cm
5			5.5–6.5cm
6			6.5–7.5cm
7			7.5–10 cm

²⁹R (²⁹N₂/²⁸N₂) and ³⁰R (³⁰N₂/²⁸N₂) N₂ isotope ratios were determined for N₂, N₂ + N₂O and N₂O in the gas samples.

Soil analysis

Destructive soil sampling was performed after five and 10 days. After five days of incubation, three replicates were removed, and the soil columns were sliced into different layers (Table 1). The thickness of the cut layers depended on the slurry treatment. After ten days, this was repeated for each treatment with the remaining three samples. Soil samples were analysed for NO₃⁻, NH₄⁺, pH (CaCl₂), ¹⁵N-NO₃⁻ (frozen samples (2 mol dm⁻³ KCl solution extracts of the soils) (Dyckmans et al. 2021), WEOC (Kalbitz et al. 2003) and water content (fresh soil samples).

Samples weighing approximately 15 g were collected from each soil layer in aluminium containers to determine the water content, and dried for 48 h at 105 °C. The gravimetric water content was derived as the difference between the initial weight of the wet soil before drying and the dry weight of the soil samples. To analyse the mineral N (NO₃⁻ and NH₄⁺) content, 50 g soil samples were extracted from each soil layer with 200 mL of 2 mol dm⁻³ KCl solution. After one hour of shaking, the solution was filtered (MN 614 14 filters, Macherey & Nagel GmbH & Co. KG, Düren, Germany). The solution was stored at -18 °C until concentration analyses were performed, and then measured by the colorimetric measurement method (SA 5000 continuous flow analyser, Skalar Analytical B.V., Breda, The Netherlands).

To calculate the relative soil-gas diffusivity, the approach of Moldrup et al. (2013) was used. For the calculation, the following equation was applied:

$$D_p/D_o = P\epsilon^X \left(\epsilon/\phi \right)^{T_a} \quad (1)$$

D_p: gas diffusion coefficient in soil (cm³ air cm⁻¹ soil s⁻¹).

D_o: gas diffusion coefficient in free air (cm² air s⁻¹).

ε: soil–air content (cm³ soil-air cm⁻³ soil).

Φ: total porosity (cm³ soil pore space cm⁻³ soil).

P (model parameter): 1.

X (model parameter): 1 + C_mΦ.

T_a (model parameter): 1.

C_m (media complexity factor): in the case of repacked soil, the value of C_m was 1.

Statistics

Statistical calculations were conducted using Python 3 (version: 3.9) (Rossum and Drake 2010) and R (version: 4.1.1) (R Core Team 2020) programming languages. The normality

of the data was tested with a Quantile–Quantile plot (Q–Q plot). To handle variance heterogeneity, cumulative N_2O_T , fp_N_2 , and fp_N_2O were log10 transformed. Cumulative emissions and mean core soil mineral N were tested with one-way analysis of variance (ANOVA) on days 5 and 10. A multiple comparison of means (Tukey HSD $p < 0.05$) was performed on the CO_2 , N_2O_T , fp_N_2 , fp_N_2O , NO_3^- , NH_4^+ , WEOC and pH data.

Results

Mineral N

Spatial and temporal changes in NO_3^- concentration

The NO_3^- -N content in the 0 to 10 cm layer of the C40 treatment without slurry remained close to the initial content of $69.15 \text{ mg N kg}^{-1}$ throughout the experiment. However, the C60 treatment showed an increase of 9.5% during the first five days and a slight decrease of up to 4.3% between day 5 and day 10 (Fig. S1, Table 2).

In the first slurry-amended layer of the S40 treatment, NO_3^- increased by $48.4 \text{ mg N kg}^{-1}$ from the initial level to day 10 (Fig. S1). Between days 5 and 10, the second and third layers showed an increase of 28.41 and $19.66 \text{ mg N kg}^{-1}$, respectively. Other layers showed just minor changes during the experiment. For S60, the first five days showed decreasing NO_3^- concentrations. The day 5 NO_3^- concentrations in layers 1, 2, and 3 decreased by 6.4, 20.6, and $19.4 \text{ mg N kg}^{-1}$, respectively. The day 5 value of layer 4 was $26.1 \text{ mg N kg}^{-1}$ above the initial value. The second five days showed increasing NO_3^- levels in the first three layers by 78, 41.6, and $22.8 \text{ mg N kg}^{-1}$, respectively.

Similar trends were observed in the first five layers for the I40 and I60 treatments. On day 5, the NO_3^- concentration of all layers was higher than the initial values. The first two layers showed only minor changes. However, layers 3 and 5 increased by 20–30 mg N kg^{-1} and layer 4 by 42 mg N kg^{-1} with both treatments. A slight increase

in NO_3^- concentration was observed in layers 6 and 7 on day 5 at I60. Between days 5 and 10, NO_3^- increased in all layers except layer 7. The highest increases were measured in layer 4 (between 22 and 25 mg N kg^{-1}) and layer 5 (between 13 and 22 mg N kg^{-1}) (Fig. S1).

The average NO_3^- concentrations of the entire soil column of the control treatments were similar. The slurry-amended columns of the different treatments were of the same magnitude (Table 2). There were significant differences between controls and the slurry treatments, but no significant differences existed among the treatments in these groups (Table 2). The NO_3^- concentration of the I60 treatment was about 13% lower than the average of the other treatments.

Spatial and temporal changes in NH_4^+ concentration

The initial NH_4^+ background of the soil was 1.4 mg N kg^{-1} . A decrease in NH_4^+ concentration was observed for C40 and C60. This decrease was characteristic for almost all untreated soils. The changes were almost negligible in absolute value due to the low initial concentration (Table S2).

The dynamics of NH_4^+ content change during the experiment was similar for the S40 and S60 treatments. Compared to the initial value, the slurry amended layer 1 showed a significant increase of NH_4^+ concentration on day 5. Concentrations were about 70–80 times higher. Between days 5 and 10, the trend changed. The NH_4^+ concentration of layer 1 decreased by 82 mg N kg^{-1} and 96 mg N kg^{-1} for S40 and S60, respectively (Table S2, Fig. S2).

For I40 and I60, the slurry amended layer (layer 4) and the adjacent layers (layers 3 and 5) had an increased NH_4^+ concentration at day 5 compared to the initial value. Between days 5 and 10, there was a decrease or no change in the concentrations of the layers. For I40 and I60, the NH_4^+ content of layer 4 increased on day 5 by 59 mg N kg^{-1} and 50 mg N kg^{-1} , respectively. Increases in layers 3 and 5 were at least 6 times smaller. At day 10,

Table 2 Measured average values of NO_3^- , NH_4^+ , WEOC and pH of the whole of each soil column after ten days' laboratory incubation of the silt loam soil with (surface and injected) and without slurry application at two WFPS (40% and 60%) levels. Averages and standard deviations of three, 10 days long incubated replicate cores without (C40 and C60) slurry and with surface-applied slurry (S40 and S60) and injected slurry (I40 and I60) are shown. Superscript letters indicate significant differences between treatments ($p < 0.05$; Tukey HSD, $n = 3$)

	NO_3^- [mg N kg^{-1}]	NH_4^+ [mg N kg^{-1}]	WEOC [mg C kg^{-1}]	pH (CaCl ₂)
C40	116.86 ± 0.23^a	0.64 ± 0.08^a	3.60 ± 0.92^{ab}	8.07 ± 0.013^{ab}
C60	121.82 ± 10.13^a	0.69 ± 0.16^a	2.47 ± 0.14^a	8.09 ± 0.026^a
S40	173.03 ± 49.76^b	14.09 ± 24.54^b	3.67 ± 1.014^{ab}	8.07 ± 0.078^{ab}
S60	168.34 ± 46.40^b	0.69 ± 0.33^a	2.91 ± 0.95^{ab}	8.01 ± 0.12^b
I40	161.38 ± 39.95^b	1.05 ± 0.99^a	3.77 ± 0.95^b	8.13 ± 0.12^a
I60	168.39 ± 34.50^b	1.33 ± 3.34^a	3.42 ± 1.14^{ab}	8.14 ± 0.12^a

the concentration decreased almost to the initial values also at I40 and I60 (Table S2).

The average NH_4^+ concentrations of the S40 treatment were 22 times higher than those of the C40 treatment (Table 2). The surface application method had a significant effect on NH_4^+ concentration. The mean NH_4^+ values of S60, I40 and I60 treatments did not show significant differences (caption of Table 2, superscript letters).

Weoc, water content, gas diffusivity and pH

Between days 5 and 10, the WEOC content in the 0 to 10 cm layer of the C40 and C60 treatments decreased by 10% and 33%, respectively.

In the S40 treatment, all layers showed a decrease in WEOC between day 5 and day 10. The first layer showed a decrease of 52% and the other layers decreased by approximately 22–36% (Fig. S3). In S60, the decrease in WEOC between day 5 and day 10 was almost 64% in the first layer and 40%, 34%, and 43% in layers 2, 3, and 4 (Fig. S3).

In I40 and I60, the WEOC of the slurry-treated layer 4 and the overlying adjacent layer 3 showed a high increase during the first five days and a substantial decrease by day 10 (Fig. S3). The WEOC of the slurry-treated layer 4 in I40 and I60 decreased by almost 50% and 24%, respectively, between day 5 and day 10. In I40 and I60, all the other layers showed a similar decrease of between 20% and 35%, with the exception of layer 3 in I60, where the decrease of the WEOC was only 5%.

The average WEOC of the C60 treatment showed a significant difference compared to the I40 treatment (Table 2). The C40, S40, I40 and I60 treatments showed similarities with each other and with the C60 and I40 treatments.

At 40% WFPS, the slurry layers' water content was slightly higher than the adjacent layers (Fig. S4_n). The adjacent layers show that the slurry's water moved to the upper (I40) or lower (S40 and I40) layers. The gravimetric water content (GWC) was lowest in C40 (Fig. S3), and was almost the same between day 5 and day 10. In C60, the GWC also did not change during the experiment. On average, the slurry-treated layers in S40 had a 7% higher GWC, and S60 had a 13% higher GWC than the underlying soil. On average, the fourth slurry-treated layer of I40 had a 14% higher GWC and I60 had a 16% higher GWC than layers 3 and 5. Gas diffusivity (D_p/D_o) was inversely correlated with GWC (Fig. S5). The pH of the control soils was 6.2 (Table 2). Except for S60, the average pH of the slurry-treated soils was not significantly different from the controls (Table 2). The pH of the slurry-treated layers was 2–9% higher than that of the

control (Fig. S6). The pH changes in the adjacent layers were negligible.

CH₄ and CO₂ fluxes

CH₄ fluxes were below the detection limit throughout the experiment. All the treatments exhibited constantly decreasing CO₂ fluxes during the experiments, which differed in the magnitude of initial and final fluxes by a maximum of 150 mg C m⁻² h⁻¹. The CO₂ flux dynamics of the control treatments' moisture levels were comparable (Fig. 1). The initial and final values of the C60 treatments were around 30% higher than those of C40. The S40 and S60 treatments had a similar emission pattern and magnitude, but S40 showed a faster decreasing trend. The initial value of S40 was 7% higher than that of S60, but the final value of S40 was about 20% lower than that of S60. The S60 treatment had smaller but more peaks between days 4 and 7 compared with the S40 treatment, where fewer but higher CO₂ emissions were detected. The emission pattern and magnitude of I40 showed similarities with C60. The maximum value of the I40 treatment was 22% smaller than the maximum value of I60. I60 showed a faster decrease trend than I40. The mean daily CO₂ flux of the slurry-treated soil at 40% WFPS showed a significant difference to that of C40 (Table 3), and this was also true for the 60% WFPS slurry treatments compared with the C60 treatments. Of the slurry-treated soils, no significant difference were identified between the slurry-treated treatments with the same water content (Table 3).

N₂O, N₂ fluxes and product ratio of denitrification

All treatments showed an overall decreasing trend during incubation. The fluxes of all treatments were lower at day 10 than at the beginning. The total N₂O flux (N₂O_T) was lowest in C40 treatment (0.11 ± 0.04 mg N m⁻² day⁻¹), and highest in the I60 treatment (13.32 ± 10.54 mg N m⁻² day⁻¹). N₂O_T was significantly and with the same magnitude (3.7 times) higher in C60 and S60 treatments than in C40 and S40 treatments (Table 3). Since the N₂O_T flux of the I40 treatment was relatively low, the flux of I60 was almost 32 times higher. The patterns were similar, but the differences were smaller for fp_N₂O, fp_N₂ and fp_N₂ + fp_N₂O, where the I60 treatment was about 16 times higher than I40. For N₂O_{os}, the average difference between the dry and wet treatments was almost 39 times higher.

The product ratio of denitrification (N₂O_i = fp_N₂O / (fp_N₂ + fp_N₂O)) was low in C40 and 3.5 times higher in C60 (Table 3). The surface 60% WFPS treatment was 44.5% lower than the dry treatment. The trend was similar but less for the injected treatments. The product ratio of denitrification with the wet treatment was 22.6%

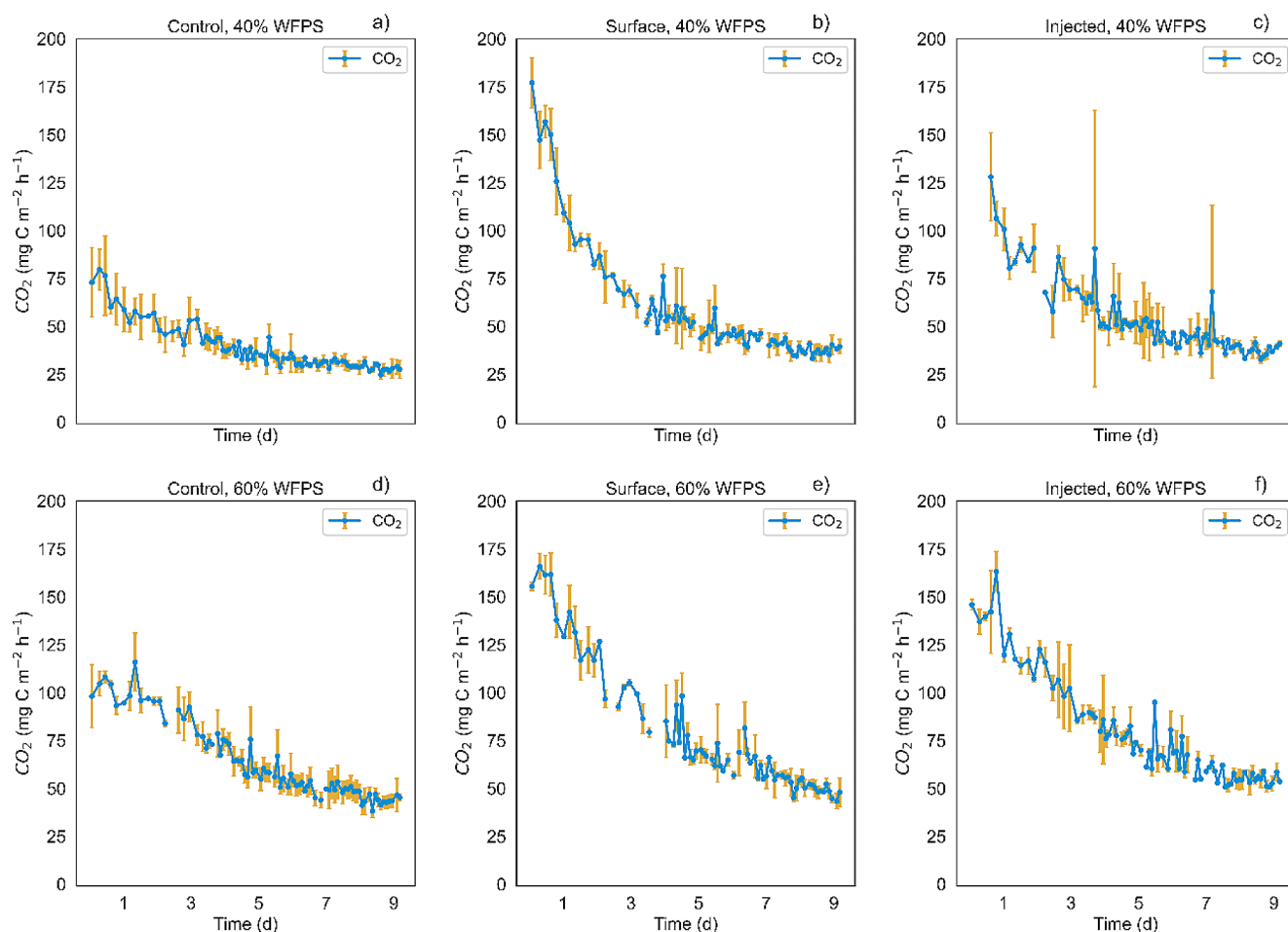


Fig. 1 CO₂ fluxes during laboratory incubation of a silt loam arable soil from Hohenheim, Germany. The water content (40% (a–c) and 60% (d–f) WFPS) was kept constant during the experiment. Three slurry treatments were applied: control (no slurry) (a,d)

(slurry on the surface) (b,e) and injected (slurry in the middle layer of the soil core) (c,f). The yellow lines represent the standard deviation of the three parallel measurements. The first visualised measurement was taken within 16 h of the soil columns being packed

Table 3 Average daily fluxes of CO₂, total N₂O (N₂O_T), N₂ (fp_N₂) and N₂O (fp_N₂O) originating from the ¹⁵N-labelled NO₃⁻ pool and N₂O from other sources (N₂O_{os}). Daily average fp_N₂ + fp_N₂O and fp_N₂ + N₂O_T (in mg N m⁻² day⁻¹; CO₂: g C m⁻² day⁻¹) and product ratio of denitrification (N₂O_i = fp_N₂O / (fp_N₂ + fp_N₂O)) are also given over a 10-day laboratory incubation of a silt loam soil with two WFPS (40% and 60%) levels. Daily averages of a 10-day experiment are shown, along with the standard deviation of three replicate cores without (C40 and C60) slurry and with surface-applied (S40 and S60) and injected (I40 and I60) slurry. Superscript letters indicate significant differences within sites and between treatments (*p* < 0.05; Tukey HSD, *n* = 3). Gaps in the flux curve represent phases when automated measurements were biased by manual gas sampling

	C40	C60	S40	S60	I40	I60
fp_N ₂	0.04 ± 0.07	0.39 ± 0.48 ^a	0.14 ± 0.11	2.88 ± 1.13 ^{ab}	0.46 ± 0.52 ^{ab}	7.83 ± 3.50 ^b
fp_N ₂ O	0.05 ± 0.09	0.48 ± 0.29 ^a	0.32 ± 0.06	1.26 ± 0.50 ^{ab}	0.74 ± 0.48 ^{ab}	11.22 ± 7.60 ^b
N ₂ O _T	0.11 ± 0.04 ^a	0.41 ± 0.21 ^b	0.38 ± 0.14 ^b	1.41 ± 0.64 ^c	0.42 ± 0.20 ^b	13.32 ± 10.54 ^d
N ₂ O _{os}	0.18 ± 0.09 ^a	0.20 ± 0.10 ^a	0.26 ± 0.10 ^a	0.54 ± 0.54 ^a	0.25 ± 0.11 ^a	9.71 ± 13.09 ^b
fp_N ₂ + fp_N ₂ O	0.13 ± 0.15	0.87 ± 0.64 ^a	0.46 ± 0.06	4.14 ± 1.58 ^{ab}	1.20 ± 0.99 ^a	19.05 ± 10.91 ^b
fp_N ₂ + N ₂ O _T	0.27 ± 0.11 ^a	1.07 ± 0.55 ^{ab}	0.72 ± 0.15 ^a	4.56 ± 1.34 ^{ab}	1.45 ± 1.03 ^{ab}	24.89 ± 11.43 ^b
N ₂ O _i	0.14	0.49 ± 0.33 ^a	0.72	0.40 ± 0.16 ^a	0.62 ± 0.12 ^a	0.48 ± 0.13 ^a
CO ₂	7.50 ± 2.57 ^a	12.27 ± 6.51 ^b	13.10 ± 4.71 ^b	13.39 ± 10.28 ^c	16.36 ± 7.02 ^b	15.90 ± 5.66 ^c

lower than with the dry treatment. The maximum difference between the C60, S60, and I60 treatments was 18.4%, but it was higher in the dry treatments. There, the difference between the dry slurry treatments was about 14%, but including C40, the maximum difference exceeded 80%.

The N_2O_T time course on a sub-daily resolution of the dry control was low throughout the experiment (Fig. 2a). The S40 and especially I40 treatments showed a higher flux and a decreasing trend. In S40, there was a slight increase between days 3 and 5, and this broad peak started to decrease after day 5 until the end of the experiment. In I40, there was a strong decrease between days 1 and 3. There were some small peaks between days 3 and 7. However, the slow decreasing trend prevailed throughout the experiment. The C60, with a small, broad peak between days 3 and 5, had a similar, but slightly higher N_2O_T flux than C40. The N_2O_T flux pattern of S60 was similar to that of S40, but the flux was significantly higher. After the greater decrease between

days 1 and 3, there was a peak on day 3, after which there was a continuous decrease until the end of the experiment. The I60 treatment had the highest N_2O_T flux compared to all other treatments. There was a rapid decrease from the beginning to day 2, and a smaller but still remarkable decrease between days 3 and 5. Despite the continuous decreasing trend, there were two small peaks on days 3 and 4.

In C40, the temporal pattern of fp_N_2O showed a small emission. In S40 and I40, the fp_N_2O had a declining trend. The fp_N_2O values of the C60, S60 and I60 treatments showed a similar pattern to those of the treatments with a water content of 40%. After the higher values on the first day, there was a decrease in the values during the rest of the experiment. In S40, I40, and S60, fp_N_2O was the dominant emitted N source on the first day. On other days and in other treatments, N_2O_{os} or fp_N_2 was similar to or more dominant than fp_N_2O . Except for the case mentioned above, N_2O_{os}

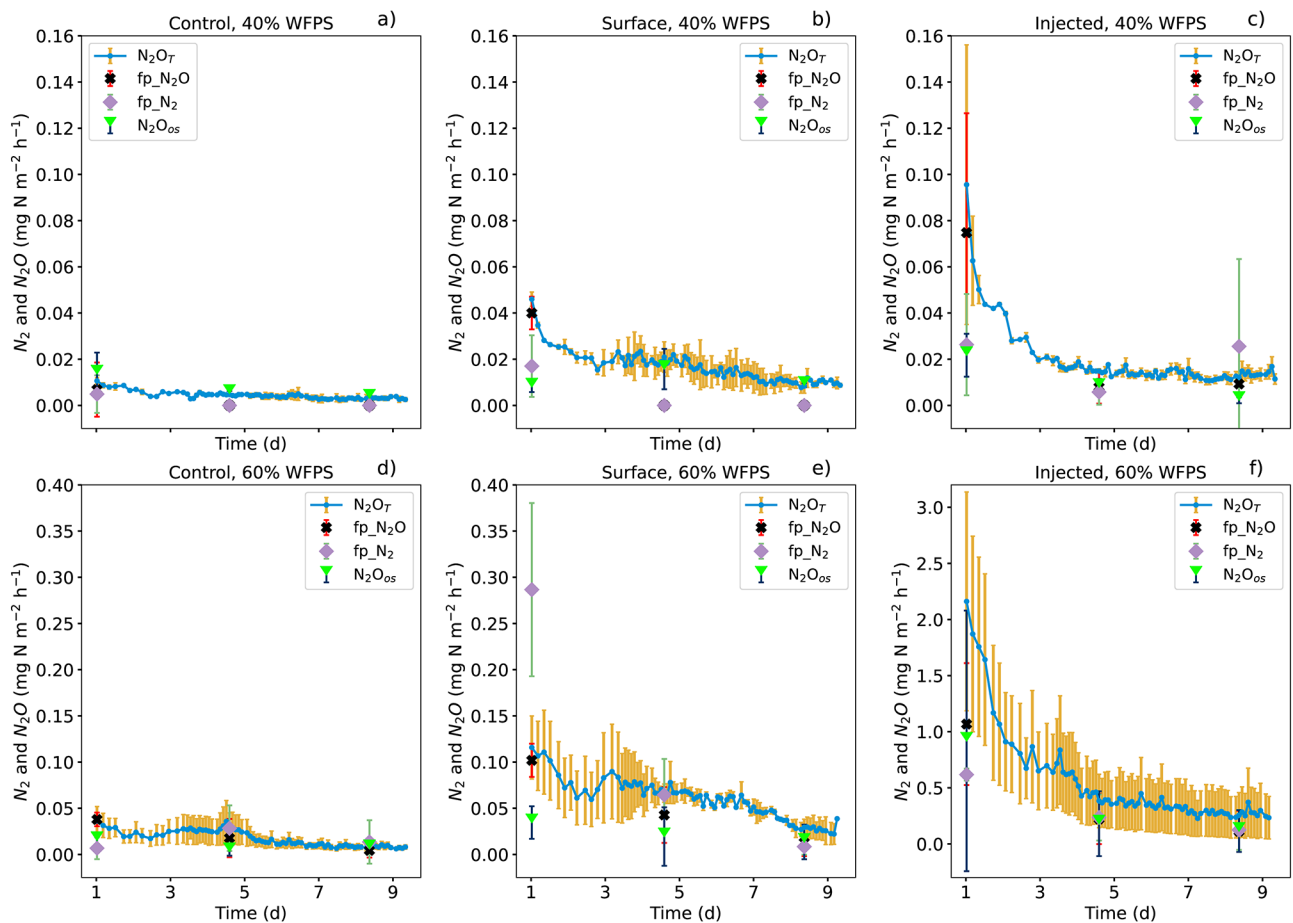


Fig. 2 Measured total N_2O flux (N_2O_T ; blue line, continuous GC measurement), fp_N_2 (purple dots; ^{15}N -sampling), fp_N_2O (black dots; ^{15}N -sampling) and N_2O_{os} (green dots; $N_2O_T - fp_N_2O$) during a laboratory incubation of silt loam, arable soil from Hohenheim, Germany. The water content (40% (a, b, c) and 60% (d, e, f) WFPS) was kept constant during the experiment. Three slurry treatments were applied:

control (no slurry) (a, c), surface-applied slurry (slurry on the surface) (b, d) and injected slurry (slurry in the middle layer of the soil) (c, f). The yellow lines represent the standard deviation of the three parallel measurements. The first visualised measurement was taken within 16 h of the soil columns being packed

and fp_N_2O were of similar magnitude. In S40, N_2O_{os} showed a slight increase on day 5.

In C40, fp_N_2 emission was low, and the trend did not change during the experiment. In S40, fp_N_2 decreased between days 1 and 5. In I40, fp_N_2 had a minimum on day 5. The fp_N_2 value on day 1 and 10 is almost the same. In C60, the temporal pattern of fp_N_2 was maximum on day 5. fp_N_2 was the dominant N source with a decreasing trend in S60 on day 1 and day 5 (Fig. 2e). The flux had a similar pattern to fp_N_2O , but tended to be higher. In I60, fp_N_2 showed a decreasing trend throughout the experiment and was below N_2O_T .

The product ratios showed a decreasing trend in all treatments except S60. The time course of N_2O_i (Fig. S6) showed that this ratio was higher in C40 and I40, but decreased during the experiment. On the first day, the N_2O_i values for S40 and I40 were almost identical. The N_2O_i values of I60 and C60 decreased during the experiment, while S60 showed the opposite trend.

The fraction originating from the $^{15}N-NO_3^-$ pool undergoing denitrification of N_2O values (Fp_N_2O) (Fig. S8) showed no trends in controls or I60, but a decreasing trend between day 1 and day 10 in S40, S60 and I40.

The denitrification source-specific N_2O fluxes (apN_2O) (Fig. S9) from the $^{15}N-NO_3^-$ enriched active pool (ap) had constant values during the experiment except for the I60 treatment, where the values decreased by almost 35% between day 1 and day 10.

Discussion

Manure effect on the depth distribution of water content, gas diffusivity, WEOC and pH

The water content in the slurry-treated and adjacent layers increased moderately in the dry and wet treatments. The moderate changes in water content in the nearby layers may be due to the silt loam soil's relatively small hydraulic conductivity and the high water-retention capacity of the slurry applied (Petersen et al. 2003; Shackelford 2003). It is important to note that this was not always the case. The hydraulic conductivity of soils can vary as a function of water content, as seen in the results for the 60% WFPS treatments. The higher water content of deeper layers in the 60% WFPS treatments can be traced back to the combined effect of higher water content resulting in increased hydraulic conductivity, the extra applied water to reach the 60% WFPS, and the water content of the applied slurry (Fig. S4).

Although the diffusion is not only dependent on the water content, there was a clear difference between the water content of the slurry-treated and adjacent layers, resulting in

a corresponding difference in calculated D_p/D_o values. The calculated D_p/D_o can be a sensitive and realistic indicator of denitrification processes (Balaine et al. 2013, 2016), while the diffusion is influenced not only by the water content of the soil, but also by the soil structure. Figure S5 shows that the diffusion of the slurry-amended layers was lower than that of the adjacent layers. This could lead to local anoxic conditions, thus enhancing denitrification, which was confirmed since N_2O and N_2 production of the soil core was elevated.

The labile C content was increased by the slurry-related WEOC in the amended soil layers, thus accelerating microbial activity, including denitrification (Baral et al. 2016). The labile C turnover is essential as a precondition for denitrification since increased respiration activity decreases the available O_2 in the soil, thereby creating anoxic conditions so that microbial denitrifiers use NO_3^- rather than O_2 as an electron acceptor (Heinen 2006; Groffman et al. 2009; Robertson and Groffman 2015). The reason for the elevated CO_2 fluxes in the surface and injected treatments, compared with the controls, may be the increased respiration of the labile organic C. The downward trend in WEOC content, especially in the slurry-treated layers, between days 5 and 10 coincided with the decreasing trend in CO_2 emissions (Fig. S3). However, the reason for the drop in WEOC concentration between days 5 and 10 could be due to both respiration and stabilisation of WEOC. The combined effect of these phenomena with the relatively high water retention of the applied slurry may be the reason for the low level of solute transport between the treated layer and adjacent or distant layers. Except for the third layer of the I60 treatments, the high WEOC content of the slurry-treated layers did not increase the WEOC concentration of the adjacent layers (Dörsch et al. 2012; Balaine et al. 2013).

The slightly higher pH of the slurry-treated layers at day 5 can be traced back to the slurry's high NH_3 , CO_3^{2-} and NH_4^+ contents (Fig. S6). NH_3 with water can form NH_4^+ in soil, and as an alkaline reaction it temporarily increases the pH. The CO_3^{2-} molecule ion can react with the soil's H^+ ions, decreasing acidity. However, the pH will slightly decrease again when NH_4^+ undergoes nitrification. One of the primary sources of the produced N_2O_{os} could be nitrification. Moreover, the relevance of nitrification was evident from the formation of NO_3^- and the reduction in NH_4^+ . It can thus be assumed that the acidifying effect of nitrification on the soil pH was not negligible.

The results mostly confirmed hypothesis (i). The water and WEOC content of the amended slurry caused increased contents of these in the adjacent soil layers after slurry application. However, it is important to note that the pH changed only in the slurry-amended soil layer, and the effect in the surrounding layers was negligible. Overall, these results

provided insight into the spatial changes in water, WEOC and pH in a silt-loam soil due to the effects of slurry. The results will help us to understand how the conditions affecting the denitrification process change. It will also allow us to integrate this new knowledge into biogeochemical models.

Manure effect on the depth distribution of mineral N

Although the changes in NH_4^+ and NO_3^- concentrations between the different treatments and dates showed similarities, there were clear differences in their magnitudes resulting from the interaction of slurry placement and soil moisture and its impact on the various N transformations (e.g., nitrification, denitrification, mineralisation, immobilisation, dissimilatory nitrate reduction to ammonium (DNRA) etc.), N gas fluxes or N leaching (Robertson and Groffman 2015).

The elevated NH_4^+ concentration in the slurry-amended layers and also in the adjacent soil layers can be explained by the NH_4^+ -N input of slurry, but also to the mineralisation of organic slurry N. The increased concentration in the nearby soil layers can be traced back to the diffusive and convective solute migration from the slurry's liquid phase. The considerable decrease in NH_4^+ content between days 5 and 10 correlated with the high fraction of N_2O flux from other sources, which, as discussed in the pH section, can be nitrification. It is important to note that the 19.3 mg NH_4^+ N kg^{-1} artificial slurry mixture added to the soil corresponds to about 210 mg NH_4^+ N kg^{-1} per 1 cm soil layer as an initial value, which decreased to about half by day 5. This decrease, in addition to the reasons mentioned above, especially in the case of surface application, could be due to the NH_3 emissivity of the slurry, which could have resulted in a significant decrease in NH_4^+ concentration (Huijsmans et al. 2003; ten Huf et al. 2023). But this could not be evaluated because measurement of NH_3 was not our goal and was not feasible with the current experimental design. Moreover, some of the decrease could also be due to immobilization. The changes in NO_3^- between days 5 and 10 inversely correlated with the changes in NH_4^+ (Figs. S1 and S2). This shows that some of the decline in NH_4^+ concentration was due to nitrification. But in view of missing NH_3 flux data and because we also did not measure N mineralisation and immobilisation, we can't quantify the share of nitrification in this decline of NH_4^+ . The increase in NO_3^- can thus probably be attributed to nitrification, which is also supported by the $\text{N}_2\text{O}_{\text{os}}$ fluxes, which had a relevant share to the total N_2O fluxes in the dry slurry treatments.

Although the calculated D_p/D_0 of the slurry-treated layers were within the range where O_2 could be limited (Petersen et al. 2013; Balaine et al. 2013), the diffusion coefficients

of the nearby soil layers were higher (Fig. S5). Therefore, the slurry-treated layer did not entirely block O_2 diffusion to deeper layers, and the nitrification process was not completely blocked. The higher NH_4^+ concentration (see Sect. Spatial and temporal changes in NH_4^+ concentration) in the slurry-treated and adjacent layers and the available O_2 created ideal conditions for nitrification (Norton and Ouyang 2019). The ideal water content for nitrification is around 40–50% WFPS (Parton et al. 2001).

Denitrification, and probably to some extent immobilization, not only increased the NO_3^- concentration but also decreased it. NO_3^- immobilization is inhibited in the presence of NH_4^+ , but not completely. The immobilization and re-mineralization of a part of the added NO_3^- – with a high amount of labile organic matter – could be important in the soil-slurry boundary layers (Schimel 1988; Davidson et al. 1991), where the concentration of WEOC is higher, but the NH_4^+ concentration is not high enough to suppress NO_3^- immobilization. At high NH_4^+ concentrations, NO_3^- immobilization is reduced to about 20% (Rice and Tiedje 1989), but at lower NH_4^+ concentrations and in the presence of WEOC, this inhibition may be reduced.

The depletion in NO_3^- content in the first three layers of the S60 treatment until day 5 could be due to the combined effect of leaching, and denitrification. The extra added water to reach 60% WFPS was below field capacity (0.32 g g^{-1}), but together with the slurry, the water content exceeded the field capacity and resulted in a vertical solute transport to the lower layers (Skaggs and Leij 2018), whereby the NO_3^- concentration did not change between days 5 and 10. Furthermore, the higher water content favoured the denitrification process, resulting in nine times higher denitrification-related $\text{N}_2 + \text{N}_2\text{O}$ gas fluxes compared with S40.

Hypothesis (ii) was confirmed since the NO_3^- concentration increased, including in nearby layers, until the end of the experiment.

Manure effect on CO_2 fluxes

The CO_2 flux of the slurry-treated soils was consistently higher than that of the controls. The enhanced respiration is due to the slurry-related labile organic C (Phan et al. 2012). But the temporal patterns of the CO_2 fluxes were probably also affected by mobilization of substrates and adaptation of the microbial community due to wetting, mixing and fertilisation during the setup of incubations. Between days 1 and 3, the CO_2 flux decreased in the controls and in all the slurry treatments. The reason for this decrease could be accounted for by the added extra water (Brinton 2020), extra NO_3^- and labile C from the slurry and from the pre-treatment of the soil (Bergstermann et al. 2011). These solutes infiltrated the soil and elevated respiration in the first few hours.

Additionally, in the slurry-treated soil, the high CO_3^{2-} concentration of the slurry could also contribute to the initial higher CO_2 flux when the soil buffers the higher pH of the slurry (Chantigny et al. 2001).

With respect to soil moisture treatments, different timing and duration of first CO_2 peaks was evident, where in the 40% WFPS treatments it came one day earlier than in the 60% treatments. The well-aerated soils had high respiration rates. However, the relatively short emission events showed that the substrate could be limited since the D_p/D_o values, even in the slurry-amended layers, were not low enough for complete O_2 limitation.

The respiration of the 60% WFPS slurry experiment was slightly higher, and the emission peaks broader, due to the better distribution of substrates by water infiltration at the higher water content. As a result, the diffusion coefficients and the available O_2 concentration were smaller, but the slurry layer's soil gas diffusion was limited. The possibility of O_2 limitation is supported by the decrease in $\text{N}_2\text{O}_{\text{os}}$ flux for both S60 and I60, possibly because nitrification was inhibited. Local O_2 depletion may have been further enhanced by O_2 consumption from respiration and nitrification. Better substrate distribution probably avoids the formation of anoxic hotspots in the layers above and below the slurry. However, it helps to build up an anaerobe volume and increase the denitrification in the slurry-amended and adjacent layers (Groffman and Tiedje 1991). The described phenomena can greatly assist in the development and tuning of the proposed slurry-soil hotspot model.

Manure effect on N_2 and N_2O processes and fluxes

Duncan et al. (2017) compared the N_2O_T flux of surface and slurry-injected soil, and the results showed that the injected slurry emitted 84–152% more N_2O_T than the surface application. Grosz et al. (2022), in a very similar experimental setup with layered slurry application, also measured a 138% higher N_2O_T flux in the injected treatment compared to the surface treatment in a laboratory incubation of sandy soil. In this experiment with silt loam soil, the 60% WFPS injected treatment measured 845% higher N_2O_T emission than the surface application. The strong injection effect of this study could be attributed to the combined effect of increased respiration, the low diffusion coefficient of the silt loam soil and especially the slurry-treated layers, and the increased NO_3^- and WEOC concentrations of the adjacent layers.

The N gas fluxes with different slurry applications and water contents (i.e. N_2O_T , fp_N_2 , $\text{fp_N}_2\text{O}$, $\text{fp_N}_2 + \text{fp_N}_2\text{O}$, $\text{N}_2\text{O}_{\text{os}}$) showed significant differences and similarities as well. In general, in the 60% WFPS experiments, denitrification was the dominant source of N_2O production due to the high soil moisture (Fig. S8) (Grundmann and Rolston 1987;

Groffman and Tiedje 1988). The N fluxes of 60% WFPS slurry treatments were several times higher than the 40% WFPS treatments. These results are in agreement with the known impact of soil moisture on denitrification (Burford and Bremner 1975; de Catanzaro and Beauchamp 1985; Bijay-singh et al. 1988; McCarty and Bremner 1993; Robertson and Groffman 2015). C60 yielded almost seven times more $\text{fp_N}_2 + \text{fp_N}_2\text{O}$ than C40.

Denitrification is strongly affected by changes in the available O_2 concentration resulting from diffusivity and respiration. It is assumed that the restriction in diffusivity needed for O_2 conditions suitable for denitrification is given as a threshold value of D_p/D_o of 0.02 (Stepniewski 1980; Petersen et al. 2013). Only the slurry-treated layers of S60, and the slurry-treated and nearby layers of I60, the D_p/D_o values were lower than 0.02 (Fig. S5) since water content of those layers was highest due to water and slurry amendment which is an explanation for the highest $\text{fp_N}_2 + \text{fp_N}_2\text{O}$ fluxes of these treatments. But the fact that C60 showed increased $\text{fp_N}_2 + \text{fp_N}_2\text{O}$ despite D_p/D_o values above 0.02 shows that this threshold value can't be seen as general threshold for denitrification. I60 exhibited higher $\text{fp_N}_2 + \text{fp_N}_2\text{O}$ than S60 despite similar D_p/D_o values of the manure layer, apparently because in S60, slurry was on the soil surface and thus in direct contact with atmospheric O_2 (Stepniewski 1980; Petersen et al. 2013).

In addition to moisture, the labile C, the properties and application method of the slurry also had a notable effect. The soluble substrates of the slurry infiltrated into the surrounding soil, increasing the respiration and N transformation processes. The 25% higher CO_2 flux of I40 compared with S40 showed increased respiration, probably because the slurry-soil interface was doubled due to the slurry injection, resulting in increased labile C migration to the nearby layers. This can lead to increased O_2 depletion and anoxic hotspot formation (Petersen et al. 2003). This induced increased denitrification, as $\text{fp_N}_2 + \text{fp_N}_2\text{O}$ was 2.6 times higher.

The magnitude of the N_2O reduction to N_2 depends on soil pH, moisture content, diffusivity, residence time and accumulation of N_2O , and the $C_{\text{org}}:\text{NO}_3^-$ ratio. It is known that low pH, increasing C_{org} availability and decreasing diffusivity would favour N_2O reduction and thus lowering of N_2O_i , while increasing NO_3^- availability would cause the opposite (Letey et al. 1980a, b; Groffman et al. 1988; Arah et al. 1991; Lessard et al. 1996; Paul 2015; Rummel et al. 2021; Grosz et al. 2022). Note that other factors may also influence N_2O reduction, such as soil Cu availability (Shen et al. 2020). Although we have not investigated the potential limitation of Cu, it plays an important role in the enzyme that catalyzes the reduction of N_2O . The slurry-amended soils increased the denitrification rate, but it did not lower

N_2O_i in all cases (Table 3). Contrary to expectations, S60 trended 20% lower N_2O_i than I60, thus the slurry injection did not lead to lower N_2O_i . The denitrification rate of the I60 treatment was 360% higher than that of S60. Although the absolute N_2O reduction rate was higher in I60, the higher N_2O_i resulted from the fact that the fp_{N_2O} increased more than fp_{N_2} . With respect to hypothesis (v), i.e. the application of injected slurry results in higher denitrification rates and lower N_2O_i compared to surface treatment, only the enhancement of denitrification rates was verified. In Grosz et al. (2022), a sandy soil was used with a similar experimental setting. In that experiment, I60 also had a higher denitrification rate than S60, and the N_2O_i value of I60 was also higher than that of S60, but with an even greater difference. The reason for the greater difference could be the higher diffusion rate of the layers above and the reduced residence time of the accumulated N_2O , compared with the present experiment. We had expected that slurry effects on moisture and labile C_{org} would lead to lowering of N_2O_i , but apparently, these effects were masked or overridden by other slurry effects which could be the higher gross N_2O production in I60 and /or the inhibition of N_2O reduction by high NO_3^- levels (Senbayram et al. 2018) which were highest in the slurry treated layers. Lowering of N_2O_i during the incubation of most treatments could be due to delayed formation of N_2O reductase and/or local depletion of NO_3^- in anoxic microsities (Fig. S7).

Besides denitrification, other soil processes also contribute to N_2O emissions (Köster et al. 2011) where the fraction of N_2O from other sources was quantified based on our ^{15}N data, but the processes that lead to these fluxes could not be distinguished. For example, it could be from autotrophic or heterotrophic nitrification or nitrifier denitrification (Müller and Clough 2014; Wrage-Mönnig et al. 2018). Autotrophic nitrification could be a significant source of N_2O_{os} since slurry-originated NH_4^+ transformed to NO_3^- . Autotrophic nitrification produces 0.5×10^{-3} to 1×10^{-3} mg N_2O -N per mg nitrified NH_4^+ -N (Hink et al. 2017). The initially added 42.9 kg NH_4^+ -N ha^{-1} could lead to an N_2O flux up to 0.2 to 0.4 mg N m^{-1} day $^{-1}$. These calculated values, except in I60, were in the same range as the N_2O_{os} fluxes of all treatments (Table 3). In S60 and I60, N_2O_{os} exceeded the calculated values, showing that other processes, such as nitrifier denitrification, denitrification coupled to nitrification or heterotrophic nitrification, could also be significant (Wrage-Mönnig et al. 2018).

The manure-induced hotspot effect in the soil

The results of this experiment demonstrated how the surface or injected slurry application-generated hotspot influenced moisture, labile C, mineral N dynamics, diffusion, pH,

nitrification, denitrification and respiration. This affected N cycling, including N_2 and N_2O by various pathways. The slurry-induced hotspot is typically formed on the slurry-saturated soil's 1–4 mm boundary layer. In this higher, slurry-related water content area, there is increased microbial activity, O_2 demand, and C and N turnover (Petersen and Andersen 1996; Frostegård et al. 1997; Groffman et al. 2009).

The slurry application elevated the labile C, NH_4^+ -N, water content, and slightly the pH in the slurry-treated and nearby layers (hypothesis (i)).

The nitrification of slurry-related NH_4^+ increased the NO_3^- concentrations. In a seven-day incubation study by Petersen et al. (1996), the limiting factor of denitrification was labile C. In some layers, the NO_3^- concentration decreased slightly in the first five days, but with WEOC (Fig. S2) it did not limit denitrification. However, it should be noted that the high WEOC concentration did not mean the limitation of labile C locally in a hotspot.

The balance of O_2 diffusion and consumption could be a limitation of denitrification. When the O_2 demand exceeded the transport through diffusion, the hotspots became anoxic and denitrification was the dominant process.

The increased NO_3^- and decreased NH_4^+ concentrations (Fig. S1 and S2) between days 5 and 10 (hypothesis (ii)) showed an elevated nitrification rate, and this result also corresponded with sufficient O_2 support through diffusion. These results showed similarities with the work of Petersen et al. (1996). The fp_{N_2O} and N_2O_{os} data strongly correlate with the conclusions of previous studies, confirming similar dynamics of nitrification coupled with denitrification in hotspots of slurry-treated soils (Nielsen et al. 1996).

The slurry-related water, labile C and NH_4^+ supply increased the O_2 consumption in the hotspots and provided locally anoxic conditions. It was ideal for denitrification, and especially in the S60 and I60 treatments, the fp_{N_2O} and fp_{N_2} flux was higher than in the control (hypothesis (iii)).

However, the N_2O reduction to N_2 and the product ratio of denitrification (N_2O_i) depend on the interactions of several factors. In addition to already well-known factors such as enhanced water, labile C or NO_3^- content, the pH, physical factors, temporal dynamic changes of N_2O reductase or residual O_2 also affect the reduction of N_2O (Butterbach-Bahl et al. 2013; Müller and Clough 2014). The extra available NO_3^- with available labile C and lower diffusivity was ideal for higher denitrification fluxes, but as shown by Qin et al. (2017) and Senbayram et al. (2022), despite high denitrification rates, high NO_3^- content inhibits N_2O reduction, since NO_3^- is the preferred electron acceptor of microbes over N_2O . Thus, when the available NO_3^- concentration exceeds the reduction capacity of denitrifiers, N_2O is

emitted from the soil without reduction and N_2O_i remains high.

The knowledge about the formation of slurry-induced hotspots and the description of the nitrification and denitrification processes that take place in these hotspots is very poor. Very little information is available on the spatial distribution of water and substrates from the slurry and on the extent of N_2 fluxes in these hotspots as a final product of denitrification. The estimation of denitrification fluxes, including N_2 fluxes, which are essential for accurate modeling (Grosz et al. 2023), is a challenge in model development and validation, especially in cases where very little data are available, e.g., the description of slurry-induced hotspots. Previously, this had been studied at the soil manure interface using special diffusion chambers (Nielsen et al. 1996; Nielsen and Revsbech 1998). But to the best of our knowledge, to date there has only been one study with slurry amendment to soil cores of defined bulk density and moisture mimicking surface application or injection of slurry to agricultural soil and including N_2 and N_2O gas flux measurements using the ^{15}N gas flux technique (Grosz et al. 2022). Similar to Grosz et al. (2022), our current data describe the first ten days of a slurry-induced hotspot effect, including spatial and temporal data on labile C, water, 14 and ^{15}N mineral N dynamics, product ratio, pH, gas fluxes such as CO_2 , N_2O_T , N_2O_{os} , fp_N_2O , nitrification, denitrification and respiration. The database of these two experiments provides a new opportunity for model developers. It can be used to test, improve and calibrate existing models or to develop new approaches and model concepts, such as considering the heterogeneous structure of soil and slurry instead of assuming homogenous distribution of substrates. Although the nature of the experiment and the data collected would allow modeling the experiment with existing models, this would not be particularly beneficial due to the inappropriate or missing approaches of the models and the lack of description of soil heterogeneity. It is more important to use the data to integrate these shortcomings into a new soil-manure sub-module, which will result in more realistic modeling. Based on the experimental design, the measured data can be directly used to develop sub-modules describing the slurry-soil hotspot effect and heterogeneity. These new sub-modules can be integrated into biogeochemical models.

It should be noted that the experiment had some limitations. The results from an experiment with one soil type do not indicate the behavior of all soil types under similar experimental conditions. The rare ^{15}N gas sampling resulted in poor temporal resolution of fp_N_2O and fp_N_2 fluxes, the experimental set-up was not appropriate for the detailed microscale research of the hotspot effect of the slurry-soil boundary layer or O_2 dynamic, and it could not investigate all the processes producing N_2O . Nevertheless, in this study,

we aimed to simulate the process dynamics of a repacked silt loam soil in the initial phase after slurry application, and thus, the short incubation period was well suited to the experimental setup without plants, which, at this initial time period, are of little relevance. To include the plant effect and the slurry effect, an extended period experiment would need to be designed (Buchen-Tschiskale et al. 2023). Surface application of slurry can release large amounts of NH_3 , which can contribute to significant N losses. NH_3 release was not measured in the experiment, but this was not the objective of the experiment. Since the data from the experiment will be used for model development, the design of the experiment should aim at gradually increasing the complexity, as this is the only way to explain the processes that cause the observed phenomena. Extended experiments with more frequent sampling using additional measurement techniques such as pore structure, spatial respiration, O_2 dynamics, NH_3 fluxes, gross N transformation and solute transport, would improve the knowledge and understanding of how the various control factors affect the formation and dynamic of soil-slurry hotspots (Müller et al. 2014; Schlüter et al. 2018; Rohe et al. 2021).

Conclusions

Few studies describe slurry-induced hotspot effects on nitrification and denitrification processes. This study provides important insights into the formation, spatial and temporal variation of the slurry-soil hotspot and its impact on the nitrification and denitrification processes. The main goal of this research was to study the effect of surface and injected slurry application techniques and a combination of two water contents of a silt loam arable soil on N_2 , N_2O and CO_2 fluxes and their control factors. In order to achieve generalizability of the observed phenomena, a silt loam soil was used here, after having performed almost the same experiment with a sandy arable soil in a previous study. The data produced by this experiment are appropriate for developing, improving and calibrating slurry-soil hotspot in biogeochemical models and testing the effect of slurry amendment. The results confirmed expectations that slurry application increases the content of water, labile C and mineral N and the demand of O_2 demand through respiration in slurry-treated and adjacent soil layers. The highest N_2 and N_2O fluxes were measured in the wet treatment with injected slurry application. An elevation in the reduction rate of N_2O to N_2 was determined in wet and slurry-treated soils. The continuous measurement of CO_2 flux, detailed spatial distribution of labile C, mineral N, water content and pH help explain the N_2 and N_2O fluxes, their pattern and their origin processes. Nevertheless, more detailed experiments including the measurement

of factors such as O₂ distribution, the pore structure of the soils or higher temporal resolutions of N₂, are needed.

Supplementary Information The online version contains supplementary material available at <https://doi.org/10.1007/s00374-024-01814-z>.

Acknowledgements This study was funded by the Deutsche Forschungsgemeinschaft (DFG)-Project number: 420651168: Modelling the Impact of Liquid Organic Fertilization and associated Application Techniques on N₂O and N₂ Emissions from Agricultural Soils (MOFANE). We thank the laboratory teams of the Institute of Soil Science, Centre for Stable Isotope Research and Analysis of Göttingen University and Thünen Institute of Climate-Smart Agriculture, Braunschweig, for support with the analyses and experiments, respectively. Specifically, we thank Martina Heuer, Ute Rieß, Jennifer Giere and Jens Dyckmans for isotopic analyses, Ute Tambor and Sabine Watsack for further analysis and sampling and Stefan Burkart for supporting automated incubations.

Author contributions B.G. and R.W. designed the experiment. B.G. and S.B. conducted the experiment. B.G. prepared the manuscript with contributions from all co-authors. All authors have read and agreed to the published version of the manuscript.

Funding This study was funded by the Deutsche Forschungsgemeinschaft (DFG)-Project number: 420651168: Modelling the Impact of Liquid Organic Fertilization and associated Application Techniques on N₂O and N₂ Emissions from Agricultural Soils (MOFANE). <https://gepris.dfg.de/gepris/projekt/420651168?language=en> (accessed on 26 January 2023).

Open Access funding enabled and organized by Projekt DEAL.

Data availability The mesocosm experiment data are available from the authors on request.

Declarations

Financial interests All authors certify that they have no affiliations with or involvement in any organization or entity with any financial interest or non-financial interest in the subject matter or materials discussed in this manuscript.

Institutional review board statement Not applicable.

Informed consent statement Not applicable.

Conflict of interest The authors declare no conflict of interest.

Open Access This article is licensed under a Creative Commons Attribution 4.0 International License, which permits use, sharing, adaptation, distribution and reproduction in any medium or format, as long as you give appropriate credit to the original author(s) and the source, provide a link to the Creative Commons licence, and indicate if changes were made. The images or other third party material in this article are included in the article's Creative Commons licence, unless indicated otherwise in a credit line to the material. If material is not included in the article's Creative Commons licence and your intended use is not permitted by statutory regulation or exceeds the permitted use, you will need to obtain permission directly from the copyright holder. To view a copy of this licence, visit <http://creativecommons.org/licenses/by/4.0/>.

References

- Arah JRM, Smith KA, Crichton IJ, Li HS (1991) Nitrous oxide production and denitrification in Scottish arable soils. *J Soil Sci* 42:351–367. <https://doi.org/10.1111/j.1365-2389.1991.tb00414.x>
- Balaine N, Clough TJ, Beare MH, Thomas SM, Meenken ED (2013) Changes in relative gas diffusivity explain Soil Nitrous Oxide Flux dynamics. *Soil Sci Soc Am J* 77:1496–1505. <https://doi.org/10.2136/sssaj2013.04.0141>
- Balaine N, Clough TJ, Beare MH, Thomas SM, Meenken ED, Ross JG (2016) Soil Gas Diffusivity Controls N₂O and N₂ emissions and their ratio. *Soil Sci Soc Am J* 80:529–540. <https://doi.org/10.2136/sssaj2015.09.0350>
- Baral KR, Arthur E, Olesen JE, Petersen SO (2016) Predicting nitrous oxide emissions from manure properties and soil moisture: an incubation experiment. *Soil Biol Biochem* 97:112–120. <https://doi.org/10.1016/j.soilbio.2016.03.005>
- Bergstermann A, Cárdenas L, Bol R, Gilliam L, Goulding K, Meijide A, Scholefield D, Vallejo A, Well R (2011) Effect of antecedent soil moisture conditions on emissions and isotopologue distribution of N₂O during denitrification. *Soil Biol Biochem* 43:240–250. <https://doi.org/10.1016/j.soilbio.2010.10.003>
- Bernal M, Bescós B, Burgos L, Bustamante MA, Clemente R, Fabri C, Flotats X, García-González MC, Herrero E, Mattachini G, Moscatelli G, Noguero J, Palatsi J, Piccinini S, Proniewicz M, Provolo G, Riaño B, Riau V, Sáez JA, Teresa M, Tey L, Torrellas M, Valli L, Ward AJ, Wisniewska H (2015) Evaluation of manure management systems in Europe. SAGA, available at: <http://hdl.handle.net/2117/88745> (last access: 31 January 2024)
- Bijay-singh, Ryden JC, Whithead DC (1988) Some relationships between denitrification potential and fractions of organic carbon in air-dried and field-moist soils. *Soil Biol Biochem* 20:737–741. [https://doi.org/10.1016/0038-0717\(88\)90160-5](https://doi.org/10.1016/0038-0717(88)90160-5)
- Brinton WF (2020) Laboratory Soil Handling affects CO₂ respiration, Amino-N and water stable aggregate results. *Agric Res Technol Open Access J* 24:556262. <https://doi.org/10.19080/ARTOAJ.2020.24.556262>
- Buchen-Tschiskale C, Well R, Flessa H (2023) Tracing nitrogen transformations during spring development of winter wheat induced by ¹⁵N labeled cattle slurry applied with different techniques. *Sci Total Environ* 871:162061. <https://doi.org/10.1016/j.scitotenv.2023.162061>
- Buckwell A, Nadeu E (2016) Nutrient recovery and reuse (NRR) in European agriculture. A review of the issues, opportunities, and actions. RISE Foundation, Brussels
- Burford JR, Bremner JM (1975) Relationships between the denitrification capacities of soils and total, water-soluble and readily decomposable soil organic matter. *Soil Biol Biochem* 7:389–394. [https://doi.org/10.1016/0038-0717\(75\)90055-3](https://doi.org/10.1016/0038-0717(75)90055-3)
- Butterbach-Bahl K, Baggs EM, Dannenmann M, Kiese R, Zechmeister-Boltensern S (2013) Nitrous oxide emissions from soils: how well do we understand the processes and their controls? *Philos Trans R Soc B Biol Sci* 368:20130122. <https://doi.org/10.1098/rstb.2013.0122>
- Chantigny MH, Rochette P, Angers DA (2001) Short-term C and N dynamics in a soil amended with pig slurry and barley straw: a field experiment. *Can J Soil Sci* 81:131–137. <https://doi.org/10.4141/S00-046>
- R Core Team (2020) R: A Language and Environment for Statistical Computing. Vienna, Austria. <http://www.R-project.org/>
- Davidson EA, Hart SC, Shanks CA, Firestone MK (1991) Measuring gross nitrogen mineralization, and nitrification by ¹⁵N isotopic pool dilution in intact soil cores. *J Soil Sci* 42:335–349. <https://doi.org/10.1111/j.1365-2389.1991.tb00413.x>

- de Catanzaro JB, Beauchamp EG (1985) The effect of some carbon substrates on denitrification rates and carbon utilization in soil. *Biol Fertil Soils* 1:183–187. <https://doi.org/10.1007/BF00257635>
- Dörsch P, Braker G, Bakken LR (2012) Community-specific pH response of denitrification: experiments with cells extracted from organic soils. *FEMS Microbiol Ecol* 79:530–541. <https://doi.org/10.1111/j.1574-6941.2011.01233.x>
- Duncan EW, Dell CJ, Kleinman PJA, Beegle DB (2017) Nitrous Oxide and Ammonia emissions from Injected and Broadcast-Applied dairy slurry. *J Environ Qual* 46:36–44. <https://doi.org/10.2134/jeq2016.05.0171>
- Dyckmans J, Eschenbach W, Langel R, Zwec L, Well R (2021) Nitrogen isotope analysis of aqueous ammonium and nitrate by membrane inlet isotope ratio mass spectrometry (MIRMS) at natural abundance levels. *Rapid Commun Mass Spectrom* 35. <https://doi.org/10.1002/rcm.9077>
- Erismann JW, Galloway J, Seitzinger S, Bleeker A, Butterbach-Bahl K (2011) Reactive nitrogen in the environment and its effect on climate change. *Curr Opin Environ Sustain* 3:281–290. <https://doi.org/10.1016/j.cosust.2011.08.012>
- Federal Ministry of Justice and Consumer Protection (2017) Düngeverordnung (DüV) Vom 26. Mai 2017. Verordnung über die Anwendung Von Düngemitteln, Bodenhilfsstoffen, Kultursubstraten Und Pflanzenschutzmitteln nach den Grundsätzen Der Guten Fachlichen Praxis Beim Düngen. Bundesanzeiger Verlag GmbH, 1–53, Bonn, available at: https://www.gesetze-im-internet.de/d_v_2017/D%3%BCV.pdf. (last access: 31 January 2024)
- Fiedler SR, Augustin J, Wrage-Mönnig N, Jurasinski G, Gusovius B, Glatzel S (2017) Potential short-term losses of N₂O and N₂ from high concentrations of biogas digestate in arable soils. *SOIL* 3:161–176. <https://doi.org/10.5194/soil-3-161-2017>
- Flessa H, Grief JM, Hofmeier M, Dittert K, Ruser R, Poddey E, Osterburg B, Poddey E, Wulf S, Pacholski A (2014) Minderung von Stickstoff-Emissionen aus der Landwirtschaft: Empfehlungen für die Praxis und aktuelle Fragen an die Wissenschaft. 2014
- Frostegård A, Petersen SO, Bååth E, Nielsen TH (1997) Dynamics of a microbial community associated with manure hot spots as revealed by phospholipid fatty acid analyses. *Appl Environ Microbiol* 63:2224–2231. <https://doi.org/10.1128/aem.63.6.2224-2231.1997>
- Galloway JN, Dentener FJ, Capone DG, Boyer EW, Howarth RW, Seitzinger SP, Asner GP, Cleveland CC, Green PA, Holland EA, Karl DM, Michaels AF, Porter JH, Townsend AR, Vörösmarty CJ (2004) Nitrogen cycles: past, Present, and Future. *Biogeochemistry* 70:153–226. <https://doi.org/10.1007/s10533-004-0370-0>
- Gilmour JT (1984) The effects of Soil properties on Nitrification and Nitrification Inhibition. *Soil Sci Soc Am J* 48:1262–1266. <https://doi.org/10.2136/sssaj1984.03615995004800060012x>
- Groffman PM, Tiedje JM (1988) Denitrification Hysteresis during Wetting and drying cycles in Soil. *Soil Sci Soc Am J* 52:1626–1629. <https://doi.org/10.2136/sssaj1988.03615995005200060022x>
- Groffman PM, Tiedje JM (1991) Relationships between denitrification, CO₂ production and air-filled porosity in soils of different texture and drainage. *Soil Biol Biochem* 23:299–302. [https://doi.org/10.1016/0038-0717\(91\)90067-T](https://doi.org/10.1016/0038-0717(91)90067-T)
- Groffman P, Tiedje J, Robertson GP, Christensen S (1988) Denitrification at different temporal and geographical scales: proximal and distal controls. pp 174–192
- Groffman PM, Butterbach-Bahl K, Fulweiler RW, Gold AJ, Morse JL, Stander EK, Tague C, Tonitto C, Vidon P (2009) Challenges to incorporating spatially and temporally explicit phenomena (hotspots and hot moments) in denitrification models. *Biogeochemistry* 93:49–77. <https://doi.org/10.1007/s10533-008-9277-5>
- Grosz B, Kemmann B, Burkart S, Petersen SO, Well R (2022) Understanding the Impact of Liquid Organic Fertilisation and Associated Application techniques on N₂, N₂O and CO₂ fluxes from agricultural soils. *Agriculture* 12:692. <https://doi.org/10.3390/agriculture12050692>
- Grosz BP, Matson A, Butterbach-Bahl K, Clough T, Davidson EA, Dechow R, DelGrosso S, Diamantopoulos E, Dörsch P, Haas E, He H, Henri CV, Hui D, Kleinedam K, Kraus D, Kuhnert M, Léonard J, Mueller C, Petersen SO, Sihi D, Vogeler I, Well R, Yeluripati JB, Zhang J, Scheer C (2023) Modeling denitrification: can we report what we don't know? *AGU advances* 4:e2023AV000990. <https://doi.org/10.1029/2023AV000990>
- Grundmann GL, Rolston DE (1987) Water function approximation to degree of anaerobiosis associated with denitrification. *Soil Sci* 144:437–441. <https://doi.org/10.1097/00010694-198712000-00008>
- Hantschel RE, Flessa H, Beese F (1994) An Automated Microcosm System for studying soil ecological processes. *Soil Sci Soc Am J* 58:401–404. <https://doi.org/10.2136/sssaj1994.03615995005800020023x>
- Heinen M (2006) Simplified denitrification models: overview and properties. *Geoderma* 133:444–463. <https://doi.org/10.1016/j.geoderma.2005.06.010>
- Hey C, Hertin J, Baron M, Dahms H, Doyle U, Dross M, Elmer C-F, Jung S, Kruse A, Kuhn T, Nabitz L, Salomon M, Schmid E, Steuer SD, Täuber S, Volkens A, Wiegand S, Wiese J (2015) SRU 2015, Stickstoff: Lösungsstrategien für Ein drängendes Umweltproblem. Sondergutachten. Sachverständigenrat für Umweltfragen (SRU). Geschäftsstelle des Sachverständigenrates für Umweltfragen, Berlin
- Hink L, Nicol GW, Prosser JI (2017) Archaea produce lower yields of N₂O than bacteria during aerobic ammonia oxidation in soil. *Environ Microbiol* 19:4829–4837. <https://doi.org/10.1111/1462-2920.13282>
- Huijsmans JFM, Hol JMG, Vermeulen GD (2003) Effect of application method, manure characteristics, weather and field conditions on ammonia volatilization from manure applied to arable land. *Atmos Environ* 37:3669–3680. [https://doi.org/10.1016/S1352-2310\(03\)00450-3](https://doi.org/10.1016/S1352-2310(03)00450-3)
- IUSS IUSS Working Group WRB, Working Group WRB (2015) 2015. World Reference Base for Soil Resources 2014, update 2015 International soil classification system for naming soils and creating legends for soil maps. World Soil Resources Reports No. 106. FAO, Rome
- John PS, Buresh RJ, Prasad R, Pandey RK (1989) Nitrogen gas (N₂ + N₂O) flux from urea applied to lowland rice as affected by green manure. *Plant Soil* 119:7–13. <https://doi.org/10.1007/BF02370264>
- Kalbitz K, Schmerwitz J, Schwesig D, Matzner E (2003) Biodegradation of soil-derived dissolved organic matter as related to its properties. *Geoderma* 113:273–291. [https://doi.org/10.1016/S0016-7061\(02\)00365-8](https://doi.org/10.1016/S0016-7061(02)00365-8)
- Kemmann B, Wöhl L, Fuß R, Schrader S, Well R, Ruf T (2021) N₂ and N₂O mitigation potential of replacing maize with the perennial biomass crop *Silphium perfoliatum* —An incubation study. *GCB Bioenergy* 13:1649–1665. <https://doi.org/10.1111/gcbb.12879>
- Königer J, Lugato E, Panagos P, Kochupillai M, Orgiazzi A, Briones MJI (2021) Manure management and soil biodiversity: towards more sustainable food systems in the EU. *Agric Syst* 194:103251. <https://doi.org/10.1016/j.agsy.2021.103251>
- Kool DM, Hoffland E, Abrahamse S, P A, van Groenigen JW (2006) What artificial urine composition is adequate for simulating soil N₂O fluxes and mineral N dynamics? *Soil Biol Biochem* 38:1757–1763. <https://doi.org/10.1016/j.soilbio.2005.11.030>
- Köster JR, Cárdenas L, Senbayram M, Bol R, Well R, Butler M, Mühling KH, Dittert K (2011) Rapid shift from denitrification to nitrification in soil after biogas residue application as indicated

- by nitrous oxide isotopomers. *Soil Biol Biochem* 43:1671–1677. <https://doi.org/10.1016/j.soilbio.2011.04.004>
- Köster JR, Cárdenas LM, Bol R, Lewicka-Szczebak D, Senbayram M, Well R, Giesemann A, Dittert K (2015) Anaerobic digestates lower N₂O emissions compared to cattle slurry by affecting rate and product stoichiometry of denitrification - an N₂O isotopomer case study. *Soil Biol Biochem* 84:65–74. <https://doi.org/10.1016/j.soilbio.2015.01.021>
- Lessard R, Rochette P, Gregorich EG, Pattey E, Desjardins RL (1996) Nitrous Oxide fluxes from Manure-Amended Soil under Maize. *J Environ Qual* 25:1371–1377. <https://doi.org/10.2134/jeq1996.004724250025000600029x>
- Letey J, Jury WA, Hadas A, Valoras N (1980a) Gas diffusion as a factor in laboratory incubation studies on Denitrification. *J Environ Qual* 9:223–227. <https://doi.org/10.2134/jeq1980.00472425000900020012x>
- Letey J, Valoras N, Hadas A, Focht DD (1980b) Effect of air-filled porosity, Nitrate concentration, and Time on the ratio of N₂O/N₂ evolution during denitrification. *J Environ Qual* 9:227–231. <https://doi.org/10.2134/jeq1980.00472425000900020013x>
- Lewicka-Szczebak D, Well R, Giesemann A, Rohe L, Wolf U (2013) An enhanced technique for automated determination of ¹⁵N signatures of N₂, (N₂+N₂O) and N₂O in gas samples. *Rapid Commun Mass Spectrom* 27:1548–1558. <https://doi.org/10.1002/rcm.6605>
- Lewicka-Szczebak D, Augustin J, Giesemann A, Well R (2017) Quantifying N₂O reduction to N₂ based on N₂O isotopocules – validation with independent methods (Helium incubation and ¹⁵N gas flux method). *Biogeosciences* 14:711–732. <https://doi.org/10.5194/bg-14-711-2017>
- Li C, Salas W, Zhang R, Krauter C, Rotz A, Mitloehner F (2012) Manure-DNDC: a biogeochemical process model for quantifying greenhouse gas and ammonia emissions from livestock manure systems. *Nutr Cycl Agroecosystems* 93:163–200. <https://doi.org/10.1007/s10705-012-9507-z>
- Malhi SS, McGill WB (1982) Nitrification in three Alberta soils: Effect of temperature, moisture and substrate concentration. *Soil Biol Biochem* 14:393–399. [https://doi.org/10.1016/0038-0717\(82\)90011-6](https://doi.org/10.1016/0038-0717(82)90011-6)
- Malyan SK, Bhatia A, Fagodiya RK, Kumar SS, Kumar A, Gupta DK, Tomer R, Harit RC, Kumar V, Jain N, Pathak H (2021a) Plummeting global warming potential by chemicals interventions in irrigated rice: a lab to field assessment. *Agric Ecosyst Environ* 319:107545. <https://doi.org/10.1016/j.agee.2021.107545>
- Malyan SK, Kumar SS, Fagodiya RK, Ghosh P, Kumar A, Singh R, Singh L (2021b) Biochar for environmental sustainability in the energy-water-agroecosystem nexus. *Renew Sustain Energy Rev* 149:111379. <https://doi.org/10.1016/j.rser.2021.111379>
- Markfoged R, Nielsen LP, Nyord T, Ottosen LDM, Revsbech NP (2011) Transient N₂O accumulation and emission caused by O₂ depletion in soil after liquid manure injection. *Eur J Soil Sci* 62:541–550. <https://doi.org/10.1111/j.1365-2389.2010.01345.x>
- McCarty GW, Bremner JM (1993) Factors affecting the availability of organic carbon for denitrification of nitrate in subsoils. *Biol Fertil Soils* 15:132–136. <https://doi.org/10.1007/BF00336431>
- Moldrup P, Chamindu Deepagoda TKK, Hamamoto S, Komatsu T, Kawamoto K, Rolston DE, Jonge LW (2013) Structure-Dependent Water-Induced Linear reduction model for Predicting Gas Diffusivity and Tortuosity in Repacked and Intact Soil. *Vadose Zone J* 12:1–11. <https://doi.org/10.2136/vzj2013.01.0026>
- Müller C, Clough TJ (2014) Advances in understanding nitrogen flows and transformations: gaps and research pathways. *J Agric Sci* 152:34–44. <https://doi.org/10.1017/S0021859613000610>
- Müller C, Laughlin RJ, Spott O, Rütting T (2014) Quantification of N₂O emission pathways via a ¹⁵N tracing model. *Soil Biol Biochem* 72:44–54. <https://doi.org/10.1016/j.soilbio.2014.01.013>
- Nielsen TH, Revsbech NP (1998) Nitrification, denitrification, and N-liberation associated with two types of organic hot-spots in soil. *Soil Biol Biochem* 30:611–619. [https://doi.org/10.1016/S0038-0717\(97\)00211-3](https://doi.org/10.1016/S0038-0717(97)00211-3)
- Nielsen TH, Nielsen LP, Revsbech NP (1996) Nitrification and coupled nitrification-denitrification Associated with a soil-manure interface. *Soil Sci Soc Am J* 60:1829–1840. <https://doi.org/10.2136/sssaj1996.03615995006000060031x>
- Norton J, Ouyang Y (2019) Controls and adaptive management of Nitrification in Agricultural soils. *Front Microbiol* 10. <https://doi.org/10.3389/fmicb.2019.01931>
- Pacholski A (2016) Calibrated Passive Sampling - Multi-plot Field measurements of NH₃ emissions with a combination of dynamic tube Method and Passive samplers. *J Vis Exp* 53273. <https://doi.org/10.3791/53273>
- Park SH, Lee BR, Jung KH, Kim TH (2018) Acidification of pig slurry effects on ammonia and nitrous oxide emissions, nitrate leaching, and perennial ryegrass regrowth as estimated by ¹⁵N-urea flux. *Asian-Australas J Anim Sci* 31:457–466. <https://doi.org/10.5713/ajas.17.0556>
- Parton WJ, Holland EA, Del Grosso SJ, Hartman MD, Martin RE, Mosier AR, Ojima DS, Schimel DS (2001) Generalized model for NO_x and N₂O emissions from soils. *J Geophys Res Atmos* 106:17403–17419. <https://doi.org/10.1029/2001JD900101>
- Paul EA (2015) *Soil microbiology, ecology and biochemistry*, 4th edition. Academic Press is an imprint of Elsevier, Waltham, MA
- Peterjohn WT (1991) Denitrification: enzyme content and activity in desert soils. *Soil Biol Biochem* 23:845–855. [https://doi.org/10.1016/0038-0717\(91\)90096-3](https://doi.org/10.1016/0038-0717(91)90096-3)
- Petersen SO, Andersen MN (1996) Influence of soil water potential and slurry type on denitrification activity. *Soil Biol Biochem* 28:977–980. [https://doi.org/10.1016/0038-0717\(96\)00067-3](https://doi.org/10.1016/0038-0717(96)00067-3)
- Petersen SO, Sommer SG (2011) Ammonia and nitrous oxide interactions: roles of manure organic matter management. *Anim Feed Sci Technol* 166–167:503–513. <https://doi.org/10.1016/j.anifeedsci.2011.04.077>
- Petersen SO, Nielsen TH, Frostegård Å, Olesen T (1996) O₂ uptake, C metabolism and denitrification associated with manure hot-spots. *Soil Biol Biochem* 28:341–349. [https://doi.org/10.1016/0038-0717\(95\)00150-6](https://doi.org/10.1016/0038-0717(95)00150-6)
- Petersen SO, Nissen HH, Lund I, Ambus P (2003) Redistribution of Slurry Components as Influenced by Injection Method, Soil, and Slurry properties. *J Environ Qual* 32:2399–2409. <https://doi.org/10.2134/jeq2003.2399>
- Petersen SO, Ambus P, Elsgaard L, Schjøning P, Olesen JE (2013) Long-term effects of cropping system on N₂O emission potential. *Soil Biol Biochem* 57:706–712. <https://doi.org/10.1016/j.soilbio.2012.08.032>
- Petersen SO, Baral KR, Arthur E (2016) Manure distribution as a predictor of N₂O emissions from soil. *Anim Prod Sci* 56:549. <https://doi.org/10.1071/AN15534>
- Phan N-T, Kim K-H, Parker D, Jeon E-C, Sa J-H, Cho C-S (2012) Effect of beef cattle manure application rate on CH₄ and CO₂ emissions. *Atmos Environ* 63:327–336. <https://doi.org/10.1016/j.atmosenv.2012.09.028>
- Probert ME (2004) The APSIM Manure Model: improvements in predictability and application to laboratory studies. *Model Nutr Manag Trop Crop Syst* 114:76–84
- Qin S, Ding K, Clough TJ, Hu C, Luo J (2017) Temporal in situ dynamics of N₂O reductase activity as affected by nitrogen fertilization and implications for the N₂O/(N₂O+N₂) product ratio and N₂O mitigation. *Biol Fertil Soils* 53:723–727. <https://doi.org/10.1007/s00374-017-1232-y>
- Ravishankara AR, Daniel JS, Portmann RW (2009) Nitrous Oxide (N₂O): the Dominant ozone-depleting substance emitted in the

- 21st Century. *Science* 326:123–125. <https://doi.org/10.1126/science.1176985>
- Rice CW, Tiedje JM (1989) Regulation of nitrate assimilation by ammonium in soils and in isolated soil microorganisms. *Soil Biol Biochem* 21:597–602. [https://doi.org/10.1016/0038-0717\(89\)90135-1](https://doi.org/10.1016/0038-0717(89)90135-1)
- Robertson GP, Groffman PM (2015) Nitrogen Transformations. In: Paul EA (Ed) *Soil Microbiology, Ecology and Biochemistry* (Fourth Edition), Fourth Edition. Academic Press, Boston, pp 421–446
- Rodrigo A, Recous S, Neel C, Mary B (1997) Modelling temperature and moisture effects on C–N transformations in soils: comparison of nine models. *Ecol Model* 102:325–339. [https://doi.org/10.1016/S0304-3800\(97\)00067-7](https://doi.org/10.1016/S0304-3800(97)00067-7)
- Rohe L, Apelt B, Vogel H-J, Well R, Wu G-M, Schlüter S (2021) Denitrification in soil as a function of oxygen availability at the microscale. *Biogeosciences* 18:1185–1201. <https://doi.org/10.5194/bg-18-1185-2021>
- Rummel PS, Well R, Pausch J, Pfeiffer B, Dittert K (2021) Carbon Availability and Nitrogen Mineralization Control Denitrification Rates and Product Stoichiometry during initial maize litter decomposition. *Appl Sci* 11:5309. <https://doi.org/10.3390/app11115309>
- Sahrawat KL (2008) Factors affecting nitrification in soils. *Commun Soil Sci Plant Anal* 39:1436–1446. <https://doi.org/10.1080/00103620802004235>
- Säurich A, Tiemeyer B, Dettmann U, Don A (2019) How do sand addition, soil moisture and nutrient status influence greenhouse gas fluxes from drained organic soils? *Soil Biol Biochem* 135:71–84. <https://doi.org/10.1016/j.soilbio.2019.04.013>
- Schimel DS (1988) Calculation of microbial growth efficiency from ^{15}N immobilization. *Biogeochemistry* 6:239–243. <https://doi.org/10.1007/BF02182998>
- Schlüter S, Henjes S, Zawallich J, Bergaust L, Horn M, Ippisch O, Vogel H-J, Dörsch P (2018) Denitrification in Soil Aggregate analogues—Effect of Aggregate size and Oxygen Diffusion. *Front Environ Sci* 6. <https://doi.org/10.3389/fenvs.2018.00017>
- Senbayram M, Well R, Bol R, Chadwick DR, Jones DL, Wu D (2018) Interaction of straw amendment and soil NO_3^- content controls fungal denitrification and denitrification product stoichiometry in a sandy soil. *Soil Biol Biochem* 126:204–212. <https://doi.org/10.1016/j.soilbio.2018.09.005>
- Senbayram M, Wei Z, Wu D, Shan J, Yan X, Well R (2022) Inhibitory effect of high nitrate on N_2O reduction is offset by long moist spells in heavily N loaded arable soils. *Biol Fertil Soils* 58:77–90. <https://doi.org/10.1007/s00374-021-01612-x>
- Shackelford CD (2003) Geoenvironmental Engineering. In: Meyers RA (ed) *Encyclopedia of Physical Science and Technology*. Elsevier, pp 601–621
- Shen W, Xue H, Gao N, Shiratori Y, Kamiya T, Fujiwara T, Isobe K, Senoo K (2020) Effects of copper on nitrous oxide (N_2O) reduction in denitrifiers and N_2O emissions from agricultural soils. *Biol Fertil Soils* 56:39–51. <https://doi.org/10.1007/s00374-019-01399-y>
- Šimek M, Cooper JE (2002) The influence of soil pH on denitrification: progress towards the understanding of this interaction over the last 50 years. *Eur J Soil Sci* 53:345–354. <https://doi.org/10.1046/j.1365-2389.2002.00461.x>
- Šimek M, Hopkins DW (1999) Regulation of potential denitrification by soil pH in long-term fertilized arable soils. *Biol Fertil Soils* 30:41–47. <https://doi.org/10.1007/s003740050585>
- Skaggs TH, Leij FJ (2018) 6.3 Solute Transport: Theoretical Background. In: ACSESS. <https://onlinelibrary.wiley.com/doi/abs/10.2136/sssabookser5.4.c56>. Accessed 12 May 2022
- Sommer SG, Petersen SO, Møller HB (2004) Algorithms for calculating methane and nitrous oxide emissions from manure management. *Nutr Cycl Agroecosystems* 69:143–154. <https://doi.org/10.1023/B:FRES.0000029678.25083.fa>
- Sørensen P (1998) Effects of storage time and straw content of cattle slurry on the mineralization of nitrogen and carbon in soil. *Biol Fertil Soils* 27:85–91. <https://doi.org/10.1007/s003740050404>
- Spott O, Russow R, Apelt B, Stange CF (2006) A ^{15}N -aided artificial atmosphere gas flow technique for online determination of soil N_2 release using the zeolite Köstrolith SX6®. *Rapid Commun Mass Spectrom* 20:3267–3274. <https://doi.org/10.1002/rcm.2722>
- Stepniewski W (1980) Oxygen-diffusion and strength as related to soil compaction. I. ODR. *Pol J Soil Sci* 13:3–13
- ten Huf M, Reinsch T, Zutz M, Essich C, Ruser R, Buchen-Tschiskale C, Flessa H, Olf H-W (2023) Effects of Liquid Manure Application techniques on Ammonia Emission and Winter Wheat Yield. *Agronomy* 13:472. <https://doi.org/10.3390/agronomy13020472>
- Tian H, Xu R, Canadell JG, Thompson RL, Winiwarter W, Suntharalingam P, Davidson EA, Ciais P, Jackson RB, Janssens-Maenhout G, Prather MJ, Regnier P, Pan N, Pan S, Peters G, Shi H, Tubiello FN, Zaehle S, Zhou F, Arneeth A, Battaglia G, Berthet S, Bopp L, Bouwman A, F, Buitenhuis ET, Chang J, Chipperfield M, P, Dangal SR, S, Dlugokencky E, Elkins JW, Eyre BD, Fu B, Hall B, Ito A, Joos F, Krummel PB, Landolfi A, Laruelle G, G, Lauerwald R, Li W, Lienert S, Maavara T, MacLeod M, Millet DB, Olin S, Patra PK, Prinn RG, Raymond PA, Ruiz DJ, van der Werf GR, Vuichard N, Wang J, Weiss RF, Wells K. C, Wilson C, Yang J, Yao Y (2020) A comprehensive quantification of global nitrous oxide sources and sinks. *Nature* 586:248–256. <https://doi.org/10.1038/s41586-020-2780-0>
- van Rossum G, Drake FL (2010) The Python language reference. Release 3.0.1 [Repr]. Python Software Foundation, Hampton, NH
- Webb J, Pain B, Bittman S, Morgan J (2010) The impacts of manure application methods on emissions of ammonia, nitrous oxide and on crop response—A review. *Agric Ecosyst Environ* 137:39–46. <https://doi.org/10.1016/j.agee.2010.01.001>
- Well R, Kurganova I, Lopesdegerenyu V, Flessa H (2006) Isotopomer signatures of soil-emitted N_2O under different moisture conditions—A microcosm study with arable loess soil. *Soil Biol Biochem* 38:2923–2933. <https://doi.org/10.1016/j.soilbio.2006.05.003>
- Wrage-Mönnig N, Horn MA, Well R, Müller C, Velthof G, Oenema O (2018) The role of nitrifier denitrification in the production of nitrous oxide revisited. *Soil Biol Biochem* 123:A3–A16. <https://doi.org/10.1016/j.soilbio.2018.03.020>
- Zhang Y, Wang R, Pan Z, Liu Y, Zheng X, Ju X, Zhang C, Butterbach-Bahl K, Huang B (2019) Fertilizer nitrogen loss via N_2 emission from calcareous soil following basal urea application of winter wheat. *Atmospheric Ocean Sci Lett* 12:91–97. <https://doi.org/10.1080/16742834.2019.1568817>
- Zhu K, Bruun S, Larsen M, Glud RN, Jensen LS (2014) Spatial oxygen distribution and Nitrous Oxide emissions from Soil after Manure Application: a Novel Approach using Planar Optodes. *J Environ Qual* 43:1809–1812. <https://doi.org/10.2134/jeq2014.03.0125>

Publisher's Note Springer Nature remains neutral with regard to jurisdictional claims in published maps and institutional affiliations.